

Multiple Modes of Calcium-induced Calcium Release in Sympathetic Neurons I: Attenuation of Endoplasmic Reticulum Ca^{2+} Accumulation at Low $[\text{Ca}^{2+}]_i$ during Weak Depolarization

MEREDITH A. ALBRECHT,¹ STEPHEN L. COLEGROVE,¹ JARIN HONGPAISAN,²
NATALIA B. PIVOVAROVA,² S. BRIAN ANDREWS,^{2*} and DAVID D. FRIEL¹

¹Department of Neuroscience, Case Western Reserve University, Cleveland, OH 44106

²Laboratory of Neurobiology, National Institute of Neurological Disorders and Stroke, NIH, Bethesda, MD 20892

ABSTRACT Many cells express ryanodine receptors (RyRs) whose activation is thought to amplify depolarization-evoked elevations in cytoplasmic Ca^{2+} concentration ($[\text{Ca}^{2+}]_i$) through a process of Ca^{2+} -induced Ca^{2+} release (CICR). In neurons, it is usually assumed that CICR triggers net Ca^{2+} release from an ER Ca^{2+} store. However, since net ER Ca^{2+} transport depends on the relative rates of Ca^{2+} uptake and release via distinct pathways, weak activation of a CICR pathway during periods of ER Ca accumulation would have a totally different effect: attenuation of Ca^{2+} accumulation. Stronger CICR activation at higher $[\text{Ca}^{2+}]_i$ could further attenuate Ca^{2+} accumulation or trigger net Ca^{2+} release, depending on the quantitative properties of the underlying Ca^{2+} transporters. This and the companion study (Hongpaisan, J., N.B. Pivovarov, S.L. Colegrove, R.D. Leapman, and D.D. Friel, and S.B. Andrews. 2001. *J. Gen. Physiol.* 118:101–112) investigate which of these CICR “modes” operate during depolarization-induced Ca^{2+} entry in sympathetic neurons. The present study focuses on small $[\text{Ca}^{2+}]_i$ elevations (less than ~ 350 nM) evoked by weak depolarization. The following two approaches were used: (1) Ca^{2+} fluxes were estimated from simultaneous measurements of $[\text{Ca}^{2+}]_i$ and I_{Ca} in fura-2-loaded cells (perforated patch conditions), and (2) total ER Ca concentrations ($[\text{Ca}]_{\text{ER}}$) were measured using X-ray microanalysis. Flux analysis revealed triggered net Ca^{2+} release during depolarization in the presence but not the absence of caffeine, and $[\text{Ca}^{2+}]_i$ responses were accelerated by SERCA inhibitors, implicating ER Ca^{2+} accumulation, which was confirmed by direct $[\text{Ca}]_{\text{ER}}$ measurements. Ryanodine abolished caffeine-induced CICR and enhanced depolarization-induced ER Ca^{2+} accumulation, indicating that activation of the CICR pathway normally attenuates ER Ca^{2+} accumulation, which is a novel mechanism for accelerating evoked $[\text{Ca}^{2+}]_i$ responses. Theory shows how such a low gain mode of CICR can operate during weak stimulation and switch to net Ca^{2+} release at high $[\text{Ca}^{2+}]_i$, a transition demonstrated in the companion study. These results emphasize the importance of the relative rates of Ca^{2+} uptake and release in defining ER contributions to depolarization-induced Ca^{2+} signals.

KEY WORDS: calcium signaling • endoplasmic reticulum • caffeine • ryanodine • electron probe X-ray microanalysis

INTRODUCTION

Calcium is an important signaling ion, and changes in Ca^{2+} concentration ($[\text{Ca}^{2+}]$) regulate diverse processes in many cellular compartments. In excitable cells, depolarization-induced Ca^{2+} entry increases $[\text{Ca}^{2+}]_i$, leading to secondary changes in $[\text{Ca}^{2+}]$ within organelles such as mitochondria and ER that regulate specific Ca^{2+} -sensitive targets within these organelles (Pozzan et al., 1994; Berridge, 1998). Although mitochondria accumulate Ca^{2+} in response to depolarization-evoked $[\text{Ca}^{2+}]_i$ elevations (Babcock and Hille, 1998), the ER has been described as either a Ca^{2+} source or sink, in some cases even in the same cell type (Friel and Tsien, 1992a; Kuba, 1994; Verkhratsky and Shmigol, 1996; Toescu, 1998).

Such disparate modes of net ER Ca^{2+} transport are expected to have very different effects on cytoplasmic and intraluminal Ca^{2+} signals, and on the processes they regulate. Nevertheless, the conditions that favor net Ca^{2+} uptake versus net release by the ER are not well understood. The direction of net ER Ca^{2+} transport depends on the relative rates of Ca^{2+} uptake and release via distinct transport pathways. ER Ca^{2+} uptake is regulated by sarco- and endoplasmic reticulum Ca ATPase (SERCA)* pumps, whereas passive Ca^{2+} release is regulated, at least in part, by Ca^{2+} release channels that are gated by elevations in $[\text{Ca}^{2+}]_i$. When the rate of Ca^{2+} uptake exceeds the rate of passive Ca^{2+} release, the ER would act as a Ca^{2+} sink, whereas if the converse is true,

Address correspondence to David Friel, Ph.D., Department of Neuroscience, Case Western Reserve University, 10900 Euclid Ave. Cleveland, OH 44106. Fax: (216) 368-4650; E-mail: ddf2@po.cwru.edu.

*Abbreviations used in this paper: t-BuBHQ, 2,5-di-(t-butyl)-1,4-hydroquinone; EDX, energy-dispersive X-ray; InsP_3 , D-*myo*-inositol 1,4,5-trisphosphate; RyR, ryanodine receptors; SERCA, sarco- and endoplasmic reticulum Ca ATPase; Tg, thapsigargin.

it would act as a Ca^{2+} source. One process by which depolarization-evoked Ca^{2+} entry is thought to trigger net ER Ca^{2+} release is CICR (Berridge, 1998).

The machinery required for CICR is present in a variety of neurons (for review see Kuba, 1994). For example, sympathetic neurons contain a Ca store that sequesters Ca via a thapsigargin (Tg)-sensitive uptake system and is discharged by caffeine in a ryanodine-sensitive manner (Lipscombe et al., 1988; Thayer et al., 1988; Friel and Tsien, 1992a; Friel, 1995), arguing that it expresses both SERCAs and ryanodine-sensitive Ca^{2+} release channels, (also known as ryanodine receptors, RyRs). Observations suggesting that $[\text{Ca}^{2+}]_i$ -dependent activation of RyRs can amplify depolarization-induced $[\text{Ca}^{2+}]_i$ elevations in these and other neurons include: (1) acceleration of $[\text{Ca}^{2+}]_i$ responses in the presence of caffeine in a ryanodine-inhibitable manner (Friel and Tsien, 1992a; Usachev and Thayer, 1997); (2) slowing of $[\text{Ca}^{2+}]_i$ responses after treatment with ryanodine (Friel and Tsien, 1992a; Hua et al., 1993; Shmigol et al., 1995; Peng, 1996); (3) a supralinear relationship between the amount of Ca^{2+} that enters the cells during depolarization and the size of the resulting $[\text{Ca}^{2+}]_i$ elevation (Hua et al., 1993; Llano et al., 1994; Shmigol et al., 1995); and (4) facilitation of depolarization-evoked $[\text{Ca}^{2+}]_i$ responses at high $[\text{Ca}^{2+}]_i$ (Hua et al., 1993; Llano et al., 1994). The first observation implicates CICR in the presence of caffeine, but the others have been taken as support for a $[\text{Ca}^{2+}]_i$ - and ryanodine-sensitive amplification system that operates even in the absence of caffeine.

Activation of a CICR pathway is usually assumed to trigger net Ca^{2+} release from the ER that amplifies depolarization-induced $[\text{Ca}^{2+}]_i$ elevations. However, theory indicates that even when such a pathway is present, small $[\text{Ca}^{2+}]_i$ elevations above the resting level may stimulate net Ca^{2+} uptake by the ER (referred to hereafter as Ca^{2+} accumulation). This would occur if the rate of Ca^{2+} uptake increases more steeply with $[\text{Ca}^{2+}]_i$ than the rate of Ca^{2+} release. In this case, weak activation of RyRs would increase the rate of passive Ca^{2+} release and, as a result, lower the rate of Ca^{2+} accumulation. This is an interesting mode of CICR since, like net CICR, it would tend to increase the impact of Ca^{2+} entry on $[\text{Ca}^{2+}]_i$, but unlike net CICR, it would occur in the context of a rise in intraluminal $[\text{Ca}^{2+}]$ concentration.

This and the companion study (see Hongpaisan et al., 2001, in this issue) address four fundamental questions about neuronal RyR-mediated CICR, using sympathetic neurons as a model system: (1) What organelle is responsible for CICR? (2) How does CICR contribute to changes in the intracellular distribution of Ca during weak depolarization in the absence of CICR modifiers like caffeine? (3) How do these changes vary as the stimulus-evoked rise in $[\text{Ca}^{2+}]_i$ becomes larger? (4) What are the spatiotemporal properties of CICR? This study exam-

ines the relationship between changes in $[\text{Ca}^{2+}]_i$ and $[\text{Ca}]_{\text{ER}}$ during weak depolarization, while the companion study (see Hongpaisan et al., 2001, in this issue) examines how stimulus-evoked changes in $[\text{Ca}]_{\text{ER}}$ vary with $[\text{Ca}^{2+}]_i$ and with proximity to the plasma membrane. Some of these results have been presented previously in abstract form (Albrecht and Friel, 1997; Hongpaisan et al., 1999).

MATERIALS AND METHODS

Cell Dissociation and Culture

Bullfrog sympathetic neurons were prepared as described previously (Colegrove et al. 2000a). All procedures conform to guidelines established by our Institutional Animal Care and Use Committees.

Cytosolic Calcium Measurements

To measure $[\text{Ca}^{2+}]_i$, cells were incubated with 3 μM Fura-2 AM in normal Ringer's for 40 min at room temperature with gentle agitation followed by rinsing. The composition of normal Ringer's was (in mM): 128 NaCl, 2 KCl, 2 CaCl_2 , 10 HEPES, 10 glucose, pH adjusted to 7.3 with NaOH. Fura-2 AM was dispensed from a 1-mM stock solution in DMSO containing 25% (wt/wt) pluronic F127 (BASF Corporation). Cells were then washed with normal Ringer's and placed on the stage of an inverted microscope (Nikon Diaphot TMD) and superfused continuously (~ 5 ml/min). Recordings began ~ 20 min after washing away Fura-2 AM, permitting de-esterification of the Ca^{2+} indicator. With this loading procedure, there is little compartmentalization of fura-2 based on the low residual fluorescence observed after cells are dialyzed with dye-free internal solution under whole-cell conditions, and the loss of fluorescence after permeabilization of the plasma membrane with digitonin (Lipscombe et al., 1988). Solution changes (~ 200 ms) were made using a system of microcapillaries (Drummond microcaps, 20 μl) mounted on a micromanipulator. Fluorescence measurements were performed as described in Colegrove et al. (2000a).

Voltage Clamp

Simultaneous measurements of depolarization-evoked $[\text{Ca}^{2+}]_i$ elevations and voltage-sensitive Ca^{2+} currents (I_{Ca}) were made under voltage clamp in Fura-2 AM loaded cells using the perforated patch technique. Patch pipettes (1–2 M Ω) were pulled (Sutter Instruments P-97), coated with Sylgard, fire-polished, and the tips were filled with a solution containing (in mM): 125 CsCl, 5 MgCl_2 , 10 HEPES, pH 7.3 with CsOH. After filling tips, pipettes were back-filled with the same solution supplemented with amphotericin B dispensed from concentrated aliquots (12 mg/100 μl DMSO) to give a final concentration of 480 $\mu\text{g}/\text{ml}$. After they were prepared, amphotericin B-containing internal solutions were kept on ice and used within 2 h. Upon achieving a high resistance seal, series resistance declined over 5–10 min to <10 M Ω . Cells were exposed to an extracellular solution containing (in mM): 130 TEACl, 10 HEPES, 10 glucose, 2 CaCl_2 , 1 MgCl_2 , pH 7.3 with TEAOH. Currents were measured with an Axopatch 200A voltage clamp (Axon instruments) using series resistance compensation ($\sim 90\%$) and were filtered at 5 kHz. Cells were held at -70 mV and depolarized to -35 mV while current and fluorescence intensity were measured at 5 kHz for 0.2 s before and after changes in voltage, and at 4–5 Hz otherwise and saved on a laboratory computer. Currents were corrected for a linear leak based on responses to small hyperpolarizing voltage steps.

Measurement of $[Ca]_{ER}$

Total Ca concentrations within structurally identified cisternae of ER ($[Ca]_{ER}$) were measured by energy-dispersive X-ray (EDX) microanalysis of freeze-dried cryosections obtained from rapidly frozen ganglia, as described previously (Pozzo-Miller et al., 1997; Pivovarova et al., 1999). In brief, dispersed ganglia were frozen by impact against a LN₂-cooled metal block (modified Life Cell CF100); subsequently, cryosections were prepared (nominal thickness ~ 80 nm) and analyzed using instrumentation described in the companion paper (see Hongpaisan et al., 2001, in this issue). For each experimental condition, individual $[Ca]_{ER}$ measurements were taken from random somatic regions from multiple cells and averaged, so that the concentrations reported should closely approximate true spatial averages. A probe size of 63 nm was used; smaller probes yielded essentially similar results, confirming that this probe was adequate to determine ER content without contamination from adjacent cytosol. Measurements are given in units of millimoles per kilogram dry weight, from which estimated concentrations in millimoles per liter of hydrated tissue are obtained after multiplying by the estimated ratio of dry weight to total wet weight within the ER (~ 0.28 ; Pozzo-Miller et al., 1997). Resting $[Ca]_{ER}$ was measured in cells from ganglia that were incubated in normal Ringer's, and depolarization-induced changes in $[Ca]_{ER}$ were measured after transferring ganglia to 30 mM K⁺ Ringers (equimolar substitution for Na⁺) for 45 or 120 s. To assess the effect of ryanodine on resting $[Ca]_{ER}$, ganglia were transferred to normal Ringer's plus 1 μ M ryanodine supplemented with 10 mM caffeine; after five minutes, ganglia were transferred to normal Ringers plus 1 μ M ryanodine without caffeine for one additional minute before rapid freezing. Measurements of depolarization-evoked changes in $[Ca^{2+}]_i$ in fura-2-loaded cultured cells show that this protocol is sufficient to inhibit caffeine-induced $[Ca^{2+}]_i$ transients and modify depolarization-induced $[Ca^{2+}]_i$ elevations (not shown). Effects of ryanodine on evoked changes in $[Ca]_{ER}$ were assessed by treating ganglia with ryanodine as described above and then exposing them to 30 K⁺ in the presence of ryanodine.

Measurement of Ca^{2+} Fluxes

The Ca^{2+} fluxes responsible for changes in $[Ca^{2+}]_i$ during and after depolarization-evoked Ca^{2+} entry were determined based on simultaneous measurements of $[Ca^{2+}]_i$ and I_{Ca} . The total Ca^{2+} flux (J_{total}) and the component of J_{total} representing Ca^{2+} entry through voltage-sensitive Ca^{2+} channels (J_{ICa}) were estimated as described below. These measurements made it possible to estimate the net Ca^{2+} flux (J_{Σ}) representing the combined activity of all other Ca^{2+} transport systems, including Ca^{2+} extrusion across the plasma membrane and uptake and release by organelles such as the ER and mitochondria. The sign of J_{Σ} provides information about Ca^{2+} release from intracellular stores: when J_{Σ} is negative, the rate of net Ca^{2+} release exceeds the combined rate of Ca^{2+} clearance; when J_{Σ} is positive, net Ca^{2+} release, if it occurs, must be slower than Ca^{2+} clearance.

The total cytosolic Ca^{2+} flux per unit volume was measured (J_{total} , in nanomolars per second) by taking the time derivative of $[Ca^{2+}]_i$ at each sample time t_i during the period of low frequency sampling according to $([Ca^{2+}]_i(t_i + \Delta t/2) - [Ca^{2+}]_i(t_i - \Delta t/2))/\Delta t$, where Δt (400–500 ms) is twice the sampling interval. During the periods of high frequency sampling immediately after depolarization and repolarization, the flux was determined by measuring the slope of a fitted exponential function. Before calculating the fluxes, the $[Ca^{2+}]_i$ measurements were smoothed four to five times with a binomial filter.

J_{total} was dissected into two components representing the rate

of Ca^{2+} entry through voltage-sensitive Ca^{2+} channels (J_{ICa}) and the composite net flux representing transport by all other systems, ($J_{\Sigma} = J_{total} - J_{ICa}$). J_{ICa} is the rate of Ca^{2+} entry per unit cytoplasmic volume divided by the ratio (κ_i^T) of changes in total cytoplasmic Ca concentration (bound plus free) that accompany small changes in $[Ca^{2+}]_i$ (Neher and Augustine, 1992; Colegrove et al., 2000a). The rate of Ca^{2+} entry per unit cytoplasmic volume was calculated from $I_{Ca}/2Fv_i$, where F is the Faraday constant and v_i is the cytoplasmic volume estimated from the measured membrane capacitance assuming hemispherical geometry to approximate the shape of adherent cells. To estimate κ_i^T , it was reasoned that during the initial moments following depolarization, before $[Ca^{2+}]_i$ has changed sufficiently to perturb basal Ca^{2+} transport, $[Ca^{2+}]_i$ should rise at a rate that depends only on the rate of Ca^{2+} entry, the cytosolic volume, and κ_i^T . Accordingly, κ_i^T was estimated as the average ratio of $I_{Ca}/2Fv_i$ to J_{total} during the early period of depolarization (from 0.24 to 1.00 s). During this time, J_{total} was insensitive to pharmacological interventions that dramatically modified Ca^{2+} transport by the caffeine-sensitive store (see Fig. 2 C, compare left and right panels, and Fig. 4, A and B), indicating that it is dominated by Ca^{2+} entry. As expected, reducing the intracellular fura-2 concentration (by reducing loading times) systematically lowered κ_i^T and increased the magnitudes of J_{total} , J_{ICa} , and J_{Σ} . However, this did not change the signs of these fluxes, indicating that Ca^{2+} buffering by fura-2 did not influence the direction of J_{Σ} .

Pharmacological Manipulation of CICR

Ryanodine was used as a tool to evaluate how CICR contributes to stimulus-evoked $[Ca^{2+}]_i$ elevations. At low concentrations (≤ 1 μ M), ryanodine inhibits Ca^{2+} -dependent RyR channel gating and increases channel open probability. At high concentrations (> 100 μ M), it causes channel block (for reviews see Coronado et al., 1994; Berridge et al., 1995; Sutko et al., 1997; Zucchi and Roncha-Testoni, 1997). To inhibit CICR, cells were exposed to ryanodine (1 μ M) and then transiently to caffeine (10 mM) in the continued presence of ryanodine. Under these conditions, caffeine elicits a transient rise in $[Ca^{2+}]_i$ like that observed in control cells, but unlike control cells, responsiveness to caffeine is not restored after caffeine is removed (Thayer et al., 1988). Caffeine opens RyRs by increasing their sensitivity to $[Ca^{2+}]_i$ (Rousseau et al., 1988), and ryanodine is thought to inhibit caffeine responsiveness by irreversibly modifying RyRs so that they are insensitive to Ca^{2+} (Rousseau et al., 1987) or have greatly increased Ca^{2+} sensitivity (Chen et al., 2001). Ryanodine was used in conjunction with caffeine because ryanodine preferentially interacts with the open channel, causing ryanodine-induced RyR modifications to be use-dependent.

Simulations

Rate equations describing Ca^{2+} extrusion across the plasma membrane (Colegrove et al., 2000b) and Ca^{2+} uptake and release by the ER were incorporated into a system of differential equations (see APPENDIX) that was solved numerically using a fourth-order Runge-Kutta routine (Boyce and DiPrima, 1969) written in Igor Pro (Wavemetrics, Inc.). Step size was 50 ms; further reductions in step size did not noticeably alter the results.

Reagents and Data Analysis

Fura-2 AM was obtained from Molecular Probes, ryanodine was obtained from RBI, t-BuBHQ was purchased from Calbiochem, and unless indicated otherwise, all other compounds were obtained from Sigma-Aldrich. Population results are expressed as mean \pm SEM and statistical significance was assessed using t test.

RESULTS

Modulation of Depolarization-evoked $[Ca^{2+}]_i$ Responses by the Caffeine-sensitive Store

Fig. 1 shows $[Ca^{2+}]_i$ responses elicited under three different conditions illustrating how the caffeine-sensitive store can influence the impact of Ca^{2+} entry on $[Ca^{2+}]_i$. Experiments were performed under voltage clamp (perforated patch conditions) so that components of the total Ca^{2+} flux representing Ca^{2+} entry and Ca^{2+} transport by other systems could be distinguished (see next section). Recordings were made using a test potential (-35 mV) close to the membrane potential established during exposure to 30 mM K^+ to facilitate comparison with previous results obtained using this K^+ concentration to stimulate Ca^{2+} entry (Friel and Tsien, 1992a). We first show how net Ca^{2+} transport by the store can influence depolarization-evoked $[Ca^{2+}]_i$ responses under conditions that favor net Ca^{2+} release or Ca^{2+} accumulation. Flux measurements are then described that provide information about CICR under control conditions and when it is modified by caffeine.

During membrane depolarization, $[Ca^{2+}]_i$ rises toward a steady level (Fig. 1, Control 1) and recovers after repolarization. Subsequent exposure to caffeine elicits a large $[Ca^{2+}]_i$ transient reflecting Ca^{2+} release from an intracellular store (Friel and Tsien, 1992a). Several observations provide information about the mechanisms of Ca^{2+} uptake and release by this store. Caffeine is ineffective after treatment with the SERCA inhibitors thapsigargin ($Tg > 20$ nM), 2,5-di-(*t*-butyl)-1,4-hydroquinone (*t*-BuBHQ, 10 – 100 μ M) or cyclopiazonic acid (100 μ M; unpublished data), each of which elicits a transient $[Ca^{2+}]_i$ rise in the absence of extracellular Ca^{2+} , indicating that Ca^{2+} uptake by the store requires SERCA activity. Caffeine is also ineffective after treatment with ryanodine (Thayer et al., 1988; Friel and Tsien, 1992a), arguing that RyRs serve as the caffeine-sensitive Ca^{2+} release pathway. Evidence will be presented in the accompanying study directly demonstrating that the caffeine-sensitive store is the ER.

When cells are depolarized in the continued presence of caffeine (Fig. 1, +Caff), $[Ca^{2+}]_i$ responses are dramatically amplified, showing an accelerated onset leading to a prominent $[Ca^{2+}]_i$ spike. The recovery that follows repolarization is also accelerated compared with the control response. Two observations suggest that amplification is caused by Ca^{2+} -induced release: (1) it is not observed after treatment with ryanodine (1 μ M; Friel and Tsien, 1992a); and (2) in the presence of caffeine, the total Ca^{2+} flux elicited by depolarization consists of two kinetically distinct components. One component resembles the flux elicited by depolarization in the absence of caffeine, whereas the other resembles the

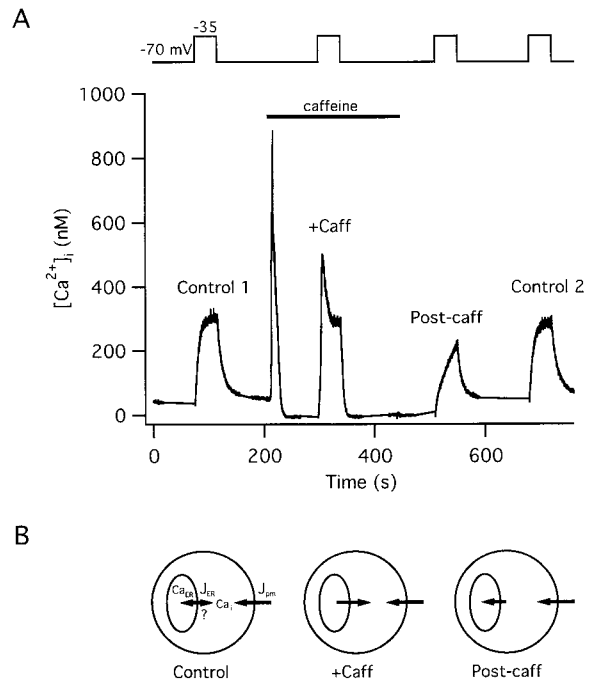


FIGURE 1. Effects of Ca^{2+} release and uptake by the caffeine-sensitive store on responses elicited by weak depolarization. $[Ca^{2+}]_i$ responses elicited from a representative cell by voltage clamp depolarization under control conditions (Control 1), during continuous exposure to 5 mM caffeine (+Caff), after removing caffeine to initiate store replenishment (Post-caff), and finally after allowing sufficient time for the store to refill (Control 2). In the presence of caffeine, depolarization-induced $[Ca^{2+}]_i$ responses are amplified, whereas during the period of replenishment after caffeine removal, responses are blunted; a final depolarization elicits a response like the control. Top trace indicates membrane potential. Exposure to the holding potential (-70 mV) (between first and second depolarizations) elicited a large $[Ca^{2+}]_i$ transient; the small reversible reduction in basal $[Ca^{2+}]_i$ seen in the presence of caffeine is due, at least in part, to an effect of caffeine on fura-2 fluorescence independent of changes in $[Ca^{2+}]_i$ (Friel and Tsien, 1992a; Muschol et al., 1999). Cell ma4441. (B) Diagrams show schematically the relationship between the net Ca^{2+} flux across the plasma membrane (J_{pm}) and between the cytosol and ER (J_{ER}) during $[Ca^{2+}]_i$ elevations elicited in the presence of caffeine (+Caff) and following caffeine washout (Post-caff). This study investigates the direction of net ER Ca^{2+} transport under control conditions.

flux underlying caffeine-induced Ca^{2+} release (Friel and Tsien, 1992b; Usachev and Thayer, 1997).

When caffeine is washed out, the store refills at a rate that depends on the availability of cytosolic Ca^{2+} and the rate of net Ca^{2+} entry across the plasma membrane (Friel and Tsien, 1992a). If cells are depolarized during this period of replenishment (Post-caff), the rise in $[Ca^{2+}]_i$ is much slower than the control, even though the underlying Ca^{2+} current is similar (not shown). Evidence has been presented previously (Friel and Tsien, 1992a) that the onset is slow because a portion of the Ca^{2+} entering through Ca^{2+} channels is taken up by the store as it refills. After allowing sufficient time for store replenishment, a final depolarization elicits a $[Ca^{2+}]_i$

response (Fig. 1, Control 2) resembling the first control response. These observations are representative of four cells studied under voltage clamp and are consistent with previous results obtained from cells depolarized with 30 mM K^+ (Friel and Tsien, 1992a). Thus, in the presence of caffeine, Ca^{2+} release via a ryanodine-sensitive pathway can amplify depolarization-induced $[Ca^{2+}]_i$ elevations; conversely, after being discharged, Ca^{2+} accumulation by the store can attenuate these responses (see diagrams, Fig. 1, bottom).

How does the caffeine-sensitive store contribute to $[Ca^{2+}]_i$ dynamics when Ca^{2+} transport is not modified by caffeine? It has been proposed that in these and other neurons, depolarization-induced $[Ca^{2+}]_i$ responses are amplified by CICR, even in the absence of caffeine. The main goal of the present study was to evaluate this possibility in a weak stimulus regime where $[Ca^{2+}]_i$ is low (less than ~ 350 nM). The companion study (see Hongpaisan et al., 2001, in this issue) examines the case where stronger stimuli raise $[Ca^{2+}]_i$ to progressively higher levels.

Components of the Total Cytosolic Ca^{2+} Flux

$[Ca^{2+}]_i$ rises during depolarization and declines after repolarization because there is a net cytoplasmic Ca^{2+} flux: inward during the onset and outward during the recovery. At each instant in time, this flux depends on the rate of stimulated Ca^{2+} entry and on the rate of endogenous Ca^{2+} transport representing, at a minimum, Ca^{2+} extrusion across the plasma membrane, and Ca^{2+} uptake and release by the ER and mitochondria. Given a measurement of the total Ca^{2+} flux and the rate of stimulated Ca^{2+} entry, the endogenous net flux can be estimated. Based on the sign of this flux, it is possible to place limits on the relative rates of net Ca^{2+} release from the caffeine-sensitive store and Ca^{2+} clearance by other transport systems.

The total cytosolic Ca^{2+} flux (J_{total} , measured in nanomoles/second) can be determined at each instant in time by measuring the time derivative of $[Ca^{2+}]_i$; this gives the rate at which Ca^{2+} leaves or enters the cytosol (e.g., in nanomoles/second) divided by the cytosolic volume and a buffering factor (κ_i^T , see MATERIALS AND METHODS). J_{total} can be separated into two components representing the net Ca^{2+} flux through voltage-sensitive Ca^{2+} channels (J_{ICa}), and the composite net flux representing endogenous Ca^{2+} transport (J_{Σ}). J_{ICa} was calculated from the measured Ca^{2+} current (I_{Ca}), the estimated cytosolic volume, and κ_i^T as described in MATERIALS AND METHODS, whereas J_{Σ} was calculated from $J_{total} - J_{ICa}$. By convention, inward fluxes that raise $[Ca^{2+}]_i$ are negative and outward fluxes that lower $[Ca^{2+}]_i$ are positive.

Fig. 2 illustrates how the interplay between J_{ICa} and J_{Σ} defines J_{total} during and after weak depolarization before

(left) and during (right) exposure to 5 mM caffeine from an experiment like that illustrated in Fig. 1. In the absence of caffeine (left column), depolarization elicits an inward Ca^{2+} current (B) causing $[Ca^{2+}]_i$ to rise (C) toward a nearly steady level. Fig. 2 D shows the time courses of J_{total} and its components during and after depolarization. During depolarization, J_{total} (Fig. 2 D, triangles) is an inward flux whose magnitude increases rapidly and then declines toward zero as $[Ca^{2+}]_i$ approaches a steady level of ~ 250 nM. After repolarization, J_{total} rapidly becomes an outward flux and then declines toward zero as $[Ca^{2+}]_i$ approaches its prestimulation level.

The temporal properties of J_{total} are defined by the interplay between J_{ICa} and J_{Σ} . The initial negative-going deflection of J_{total} after depolarization reflects rapid activation of J_{ICa} (continuous curve), whereas the later decay reflects the slow development of an opposing outward flux (J_{Σ} , circles) that nearly balances J_{ICa} by the end of the depolarization, accounting for the decline in J_{total} and the approach of $[Ca^{2+}]_i$ to a steady value. Importantly, J_{Σ} is positive under these conditions of stimulation, indicating that if the stimulus triggers net Ca^{2+} release from the caffeine-sensitive store, the rate of release must be slower than the rate of Ca^{2+} clearance by all other transport systems. Following repolarization, Ca^{2+} channel deactivation causes J_{ICa} to fall rapidly to zero, unmasking the outward flux J_{Σ} that causes $[Ca^{2+}]_i$ to decline.

Fig. 2 E plots J_{total} versus $[Ca^{2+}]_i$ during the response onset and recovery, showing the abrupt negative-going transition that follows depolarization ("On" arrow) and the decline to zero as $[Ca^{2+}]_i$ approaches a new steady level after depolarization, as well as the abrupt positive-going transition after repolarization ("Off" arrow) followed by a decline to zero as $[Ca^{2+}]_i$ returns to its prestimulation value. Fig. 2 F plots J_{Σ} against $[Ca^{2+}]_i$, showing that this flux depends weakly on $[Ca^{2+}]_i$, and for a given $[Ca^{2+}]_i$ level, has similar values during the onset and recovery, indicating that J_{Σ} , and the collective activity of the underlying transporters, do not depend strongly on I_{Ca} or voltage.

In the presence of caffeine (Fig. 2, right column), the Ca^{2+} fluxes underlying the $[Ca^{2+}]_i$ response are strikingly different. Although initially J_{total} resembles the control flux, it becomes an explosively increasing inward flux, reaching nearly -70 nM/s after which it declines and changes sign to become a transient outward flux before finally approaching zero. The large transient inward flux is responsible for the upstroke and overshoot during the $[Ca^{2+}]_i$ response, and the transient outward flux is responsible for the $[Ca^{2+}]_i$ decay from its peak to the steady level. The complex kinetics of J_{total} cannot be explained by caffeine-induced changes in J_{ICa} since this flux is similar to the control flux, except for a small but consistent depression when

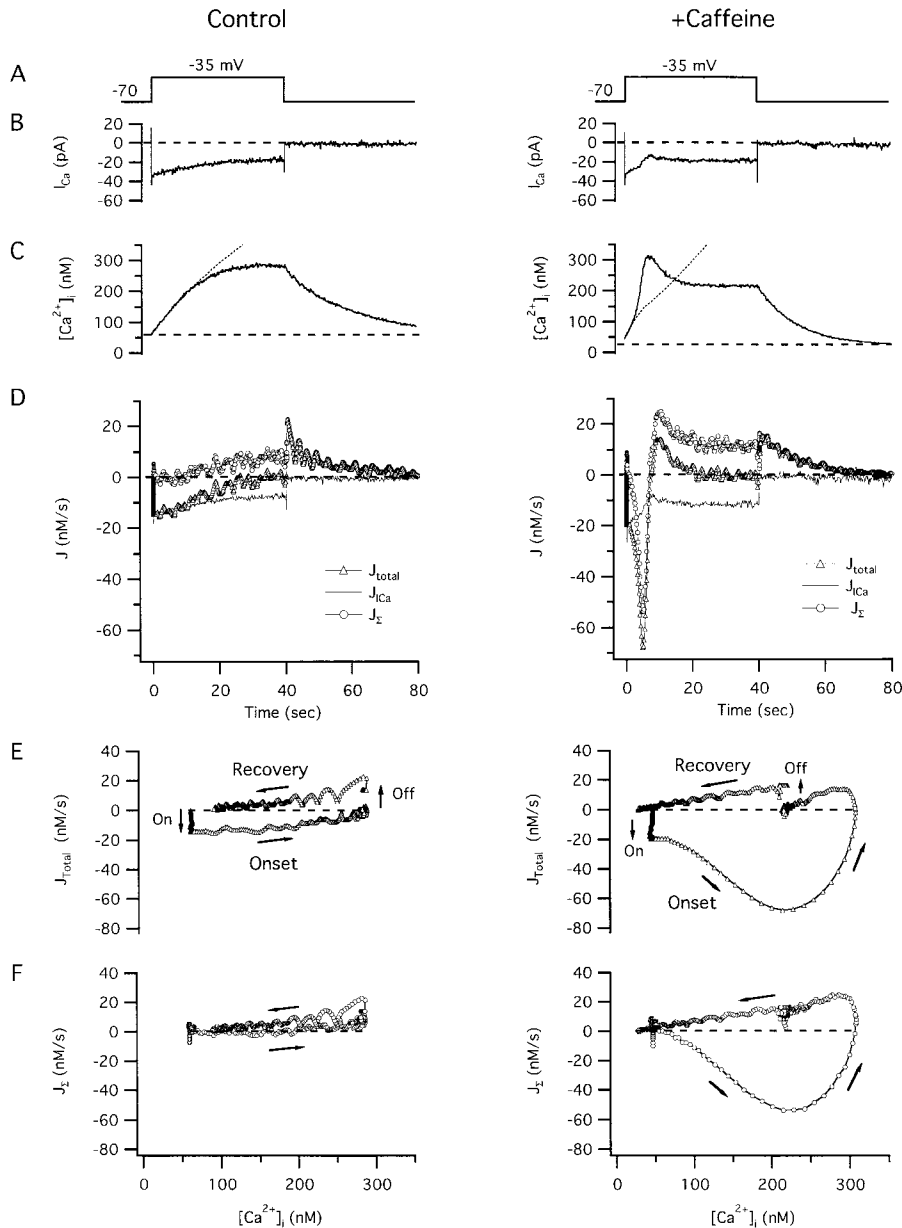


FIGURE 2. Two components of the total Ca^{2+} flux responsible for depolarization-induced changes in $[Ca^{2+}]_i$ and their modification by caffeine. Responses elicited under voltage clamp from the same cell before (left column) and during (right column) exposure to 5 mM caffeine. Panels show (A) voltage protocol, (B) I_{Ca} , (C) $[Ca^{2+}]_i$, (D) J_{total} (triangles) and its components J_{ICa} (continuous curve) and J_{Σ} (circles) all plotted on the same time scale, whereas E and F show J_{total} and J_{Σ} plotted against $[Ca^{2+}]_i$ during and after depolarization. In E and F, arrows indicate the direction of the flux trajectories as $[Ca^{2+}]_i$ changes during the response onset and recovery. Caffeine elicited a transient $[Ca^{2+}]_i$ rise (not shown) when applied between the two depolarization-evoked $[Ca^{2+}]_i$ responses illustrated here, as in Fig. 1. Dotted traces in C show integrated J_{ICa} , indicating that $[Ca^{2+}]_i$ initially rises at a rate that is proportional to I_{Ca} , but then rises more slowly than the integrated flux in the absence of caffeine, and more rapidly in its presence. Fluxes were calculated as described in MATERIALS AND METHODS. Cell ma4460.

$[Ca^{2+}]_i$ is highest. This depression may represent $[Ca^{2+}]_i$ -dependent inhibition of I_{Ca} , a contaminating outward current carried by Cs^+ through incompletely blocked Ca^{2+} -activated K^+ channels, or a combination of the two. Caffeine did not systematically influence the impact of I_{Ca} on J_{total} during the initial period of depolarization: $\kappa_i^T = 263.5 \pm 31.4$ in the presence of caffeine and 244.2 ± 38.8 in the control (four cells, NS).

The temporal properties of J_{Σ} account for the complicated dynamics of J_{total} and $[Ca^{2+}]_i$ during depolarization in the presence of caffeine. J_{Σ} consists of a large, inward spike, a transient outward component, and a steady-state component similar to that seen in the absence of caffeine. Since J_{Σ} is negative during the upstroke of the $[Ca^{2+}]_i$ spike, the rate of Ca^{2+} release must

exceed the rate of Ca^{2+} clearance, and therefore the rise in $[Ca^{2+}]_i$ would be expected to continue even if the cell were repolarized during this phase of the response (Usachev and Thayer, 1997). When repolarization occurs after $[Ca^{2+}]_i$ stabilizes and J_{Σ} is positive, $[Ca^{2+}]_i$ declines toward the prestimulation level. J_{total} and J_{Σ} are plotted against $[Ca^{2+}]_i$ for comparison with the control response (Fig. 2, E and F, right). In the presence of caffeine, J_{Σ} follows a continuous trajectory without abrupt changes in magnitude at the instants of depolarization and repolarization. This argues that in the presence of caffeine, as in the control, J_{Σ} is not very sensitive to voltage but is controlled by other variables, such as $[Ca^{2+}]_i$ and the free Ca concentration within the caffeine-sensitive store. Since J_{Σ} follows a trajectory during and after depolarization like

that followed by J_{total} during caffeine-induced Ca^{2+} release (Friel and Tsien, 1992b), it appears that the component of J_{total} responsible for response amplification in the presence of caffeine is similar to the flux responsible for caffeine-induced Ca^{2+} release, namely, CICR. Similar results were obtained in each of four cells using the same stimulus protocol.

To summarize, depolarization elicits a rise in $[\text{Ca}^{2+}]_i$, whose temporal properties reflect the interplay between voltage-sensitive Ca^{2+} entry and a composite net Ca^{2+} flux representing all other functional Ca^{2+} transport pathways. Under control conditions, the composite flux is outwardly directed, opposes the effects of Ca^{2+} entry on $[\text{Ca}^{2+}]_i$, shows little or no hysteresis, and is kinetically simple. In the presence of caffeine, the composite flux is biphasic, amplifies the effects of Ca^{2+} entry, shows strong hysteresis, and consists of a rapid transient inward component followed by a transient outward flux, having an overall trajectory resembling J_{total} after exposure to caffeine, even though the proximal stimulus is membrane depolarization, not caffeine. These observations lead to our first two important conclusions. First, when Ca^{2+} entry is stimulated in the presence of caffeine (5 mM), net Ca^{2+} release from the store occurs at a sufficiently high rate that it overwhelms available Ca^{2+} clearance systems, causing J_{Σ} to be an inward net flux. Second, if Ca^{2+} entry triggers net Ca^{2+} release from the store in the absence of caffeine, the rate of release must be less than the rate of Ca^{2+} clearance by other transport systems; otherwise, J_{Σ} would be an inward flux.

During Weak Depolarization, the Caffeine-sensitive (ER) Store Accumulates Calcium

Does the caffeine-sensitive store release net Ca^{2+} in response to depolarization-induced Ca^{2+} entry in the absence of caffeine? To examine this point, cells were depolarized before and after treatment with thapsigargin (Tg), which discharges the caffeine-sensitive store and elicits a transient $[\text{Ca}^{2+}]_i$ rise in these cells (Friel, 1995). If Ca^{2+} entry normally triggers net Ca^{2+} release, then after Tg treatment and depletion of the store, Ca^{2+} entry should elicit a $[\text{Ca}^{2+}]_i$ rise that is slower than the control. Just the opposite was observed: depolarization-evoked $[\text{Ca}^{2+}]_i$ elevations were faster after Tg (Fig. 3 A, top). This was quantified by calculating the time for $[\text{Ca}^{2+}]_i$ to rise from 20–80% of its peak value during depolarization, which after Tg treatment was reduced to $67 \pm 8\%$ of the control value ($n = 10$, $P < 0.005$). Acceleration of the depolarization-induced $[\text{Ca}^{2+}]_i$ responses could not be explained by Tg-induced enhancement of I_{Ca} (Fig. 3 A, bottom).

Treatment with Tg similarly modified $[\text{Ca}^{2+}]_i$ responses elicited by 30 mM K^+ depolarization (Fig. 3 B), leading to a reduction in the 20–80% rise time to 74%

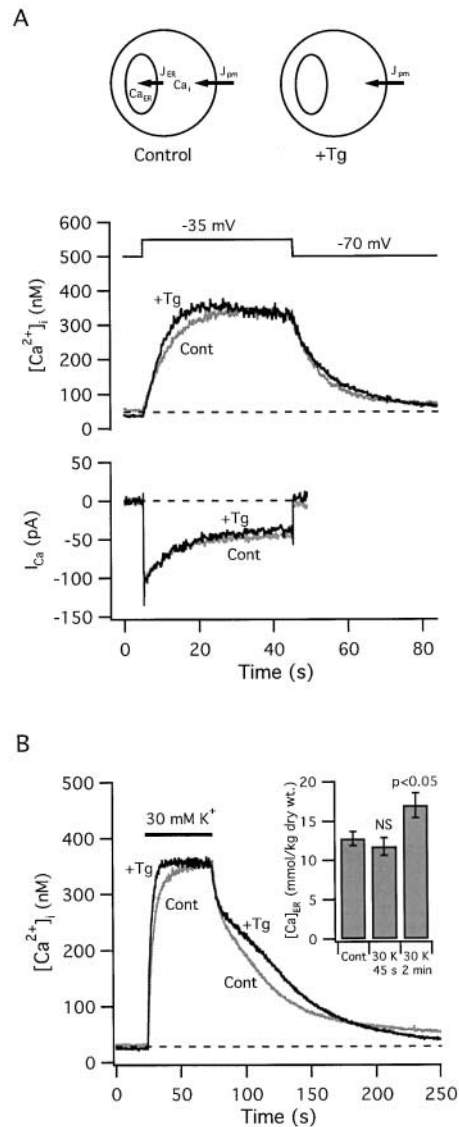


FIGURE 3. The thapsigargin-sensitive store accumulates Ca^{2+} during weak depolarization. (A) $[\text{Ca}^{2+}]_i$ responses elicited by step depolarizations from -70 to -35 mV before (light trace) and after exposure to Tg (200 nM; dark trace). In each case, depolarization elicited similar voltage-sensitive Ca^{2+} currents (bottom), but $[\text{Ca}^{2+}]_i$ increased more rapidly and reached its peak earlier after Tg treatment, supporting the conclusion that the Tg-sensitive store accumulates Ca^{2+} during these stimuli. Cell ma4620. Tg elicited a transient $[\text{Ca}^{2+}]_i$ elevation between these responses (not shown). (B) Response acceleration after Tg treatment was also seen in cells during exposure to 30 mM K^+ , which depolarizes V_m to approximately the same potential (-35 mV). This cell also illustrates a slow phase of recovery that was observed in some cells after Tg treatment under these conditions of stimulation. Inset to B shows collected results from EDX microanalysis demonstrating that exposure to 30 mM K^+ (2 min.) elevates $[\text{Ca}]_{\text{ER}}$. Diagrams in A (top) summarize the finding that during periods of Ca^{2+} entry the ER accumulates Ca^{2+} , which reduces the total cytoplasmic Ca^{2+} flux, an effect that is overcome by inhibiting Ca^{2+} uptake with Tg.

of the control value ($n = 9$, $P < 0.05$). After Tg treatment, some cells exhibited a plateau during the recovery (Fig. 3 B). The plateau appears to reflect Ca^{2+} release from mitochondria that become loaded during depolarization because it is not observed under conditions where mitochondrial Ca^{2+} release via the $\text{Na}^+/\text{Ca}^{2+}$ exchanger is inhibited, e.g., during exposure to CGP 37157 (3/3 cells, not shown; Colegrove et al., 2000a) or under voltage clamp using pipette solutions that lack Na^+ (Fig. 3 A), or in cells that respond to weak depolarization with small $[\text{Ca}^{2+}]_i$ elevations (less than ~ 250 nM; see Fig. 4 A) that should be relatively ineffective in stimulating mitochondrial Ca^{2+} accumulation (Colegrove et al., 2000a). One possible explanation is that by inhibiting ER Ca^{2+} accumulation and accelerating the rise in $[\text{Ca}^{2+}]_i$, Tg lengthens the period during which $[\text{Ca}^{2+}]_i$ is at levels that support stronger mitochondrial Ca^{2+} uptake, leading to increased loading and a more prominent plateau during the recovery.

These results suggest that the caffeine-sensitive pool accumulates Ca^{2+} when $[\text{Ca}^{2+}]_i$ is elevated during weak depolarization. This was demonstrated directly by measuring $[\text{Ca}]_{\text{ER}}$ before and after exposure to 30 mM K^+ by EDX microanalysis (Fig. 3 B, inset). $[\text{Ca}]_{\text{ER}}$ was increased significantly from its resting value during a 2 min exposure to 30 mM K^+ ; the increase corresponds to a rise from ~ 3.6 to ~ 4.8 mmol/liter wet tissue. No change in $[\text{Ca}]_{\text{ER}}$ was detected at 45 s, possibly because average $[\text{Ca}]_{\text{ER}}$ measurements before and after stimulation were necessarily performed in different cell populations, whereas ratios of 20–80% rise times were determined in individual cells and then averaged. As a result, $[\text{Ca}]_{\text{ER}}$ comparisons are more sensitive to cell-to-cell variability. A possibility that is consistent with our data is that $[\text{Ca}]_{\text{ER}}$ rises continuously during weak depolarization, being large enough at 120 s to be distinguished from basal $[\text{Ca}]_{\text{ER}}$ measurements in a different cell population, but not at 45 s. Simulations supporting this possibility are presented below (see Fig. 5 A, third panel from top).

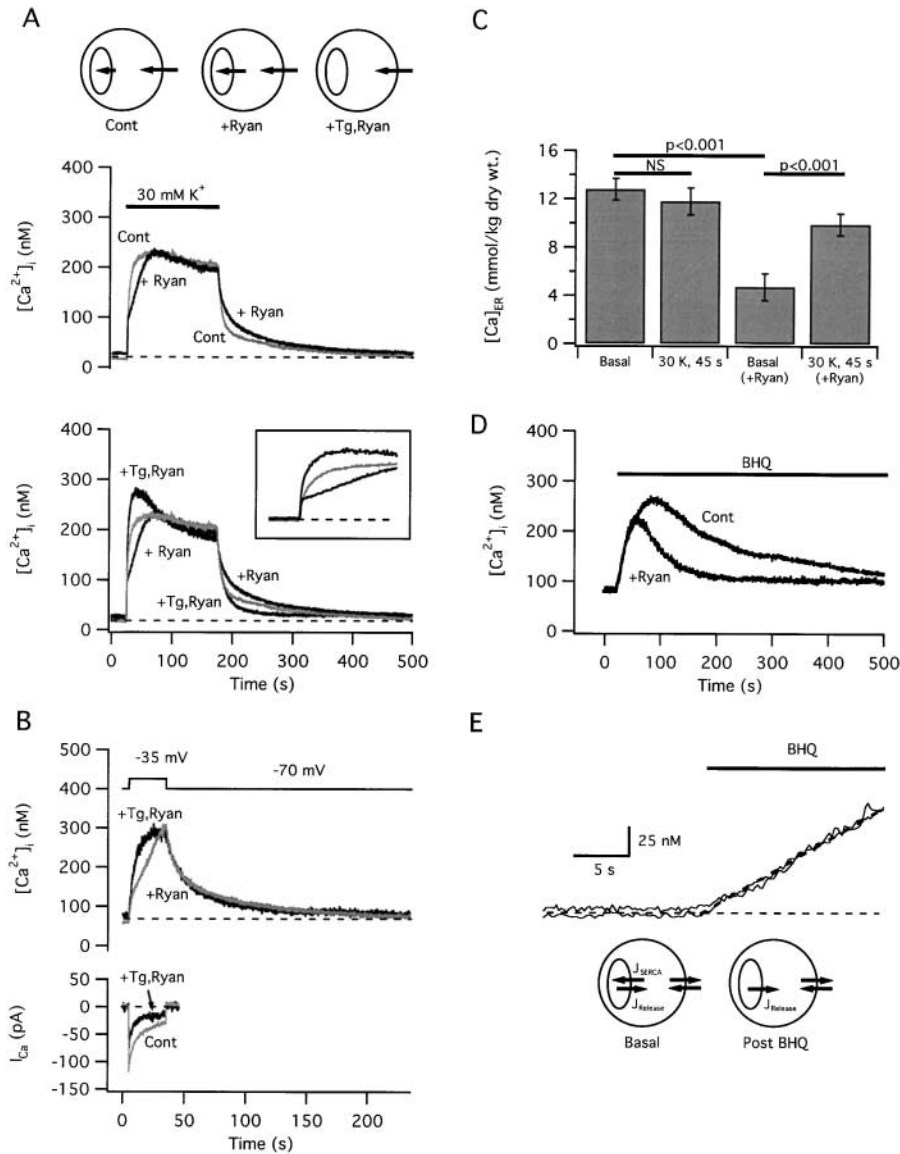
To summarize, our results indicate that Ca^{2+} accumulation by the ER reduces the total cytoplasmic Ca^{2+} flux during periods of Ca^{2+} entry and slows depolarization-evoked $[\text{Ca}^{2+}]_i$ elevations in a Tg-sensitive manner (Fig. 3 A, top, diagrams). This leads to our third important conclusion: if a ryanodine-sensitive CICR pathway is activated by the small $[\text{Ca}^{2+}]_i$ elevations elicited during weak depolarization, the rate at which Ca^{2+} is released by this pathway must be slower than the rate of Ca^{2+} uptake.

Ryanodine Slows Depolarization-evoked $[\text{Ca}^{2+}]_i$ Elevations by Enhancing ER Ca Accumulation

The results presented so far indicate that when $[\text{Ca}^{2+}]_i$ rises to levels below ~ 350 nM during weak depolarization, the caffeine-sensitive store accumulates Ca. Nevertheless, $[\text{Ca}^{2+}]_i$ responses elicited by such stimuli are

sensitive to ryanodine in a way that implicates the activation of a CICR pathway. After treatment with ryanodine, caffeine-induced Ca^{2+} release is inhibited and stimulus-induced $[\text{Ca}^{2+}]_i$ elevations are slowed (Fig. 4 A; also see Friel and Tsien, 1992a), showing a $264 \pm 21\%$ increase in the 20–80% rise time compared with control responses in the same cells (21 cells). Slower $[\text{Ca}^{2+}]_i$ elevations would account for the observation that responses induced by brief stimuli are smaller after treatment with ryanodine (Hua et al., 1993; Shmigol et al., 1995; Peng, 1996; Sandler and Barbara, 1999). At the concentrations used, ryanodine does not inhibit voltage-sensitive Ca^{2+} currents or change the initial rate at which $[\text{Ca}^{2+}]_i$ rises after depolarization (Friel and Tsien, 1992a; Fig. 4 A, bottom, inset). Moreover, ryanodine has no detectable effect after treatment with Tg (5/5 cells), indicating that it specifically influences Ca^{2+} transport by a Tg-sensitive pool. One possible explanation for the slower $[\text{Ca}^{2+}]_i$ elevations observed after treatment with ryanodine is that depolarization normally triggers net Ca^{2+} release, and that by increasing the Ca^{2+} permeability of the ER, ryanodine depletes the store, thereby preventing net Ca^{2+} release. However, this is incompatible with the observation described above that the store accumulates Ca^{2+} during weak depolarization. Another possibility is that ryanodine prevents Ca^{2+} -dependent activation of a CICR pathway that normally accelerates depolarization-induced $[\text{Ca}^{2+}]_i$ elevations, but the same observations preclude net CICR. How can these findings be explained?

Interpretation of the kinetic effects of ryanodine on depolarization-evoked $[\text{Ca}^{2+}]_i$ elevations requires information about how this compound modifies Ca^{2+} handling by the ER in these experiments. It has been shown previously that at high concentrations (≥ 10 μM), ryanodine enhances Ca^{2+} accumulation by cardiac sarcoplasmic reticulum in a way that is consistent with a reduction in sarcoplasmic reticulum Ca^{2+} permeability (Jones et al., 1979; Sutko et al., 1997). If ryanodine slows depolarization-induced $[\text{Ca}^{2+}]_i$ elevations in sympathetic neurons by a similar mechanism, then Tg should overcome this effect, causing responses to be faster than the controls (Fig. 3). Alternatively, if ryanodine renders the ER so leaky that Ca^{2+} becomes passively distributed between the ER and cytoplasm, active Ca^{2+} accumulation could not occur and Tg would have no additional effect. Fig. 4 A (bottom) compares the $[\text{Ca}^{2+}]_i$ responses from A (top) with a subsequent response elicited from the same cell after treatment with Tg in the continued presence of ryanodine. After Tg, the rise in $[\text{Ca}^{2+}]_i$ was greatly accelerated, with the 20–80% rise time falling to $36 \pm 4\%$ of that observed after treatment with ryanodine in the same cells ($n = 21$). Acceleration of the $[\text{Ca}^{2+}]_i$ rise does not reflect drug-induced changes in I_{Ca} (Fig. 4 B); in the example



μM) elicits a [Ca²⁺]_i transient whose initial rate is not influenced by ryanodine but whose amplitude and duration are altered as expected based on the ryanodine-induced reduction in [Ca]_{ER}. Cell maaa65. (E) The initial portions of the responses in D are shown on an expanded scale to illustrate the insensitivity of the initial rate to ryanodine. Diagram below shows the relationship between ER and plasma membrane Ca²⁺ fluxes under basal conditions (left) and just after inhibiting SERCAs by exposure to t-BuBHQ. Our interpretation of these results is illustrated in A (top).

shown, [Ca²⁺]_i rises more rapidly after Tg treatment despite partial rundown of I_{Ca} during the period between depolarizations. To test directly if ryanodine increases the rate of ER Ca accumulation during stimulation, a comparison was made between [Ca]_{ER} after a 45-s exposure to 30 mM K⁺ in control and ryanodine-treated cells. Although depolarization of this duration did not change [Ca]_{ER} detectably in control cells (Fig. 4 C, compare first and second bars), it increased [Ca]_{ER} twofold in ryanodine-treated cells (Fig. 4 C, compare third and fourth bars), demonstrating that ryanodine increases the average rate of ER Ca accumulation during stimulation.

Is enhanced Ca accumulation a consequence of reduced ER Ca²⁺ permeability? Such an effect by itself would cause basal [Ca]_{ER} to increase, but a ~63% reduction was observed (from 12.8 ± 0.9 to 4.7 ± 1.1 mmol/kg dry weight, *P* < 0.001; see Fig. 4 C, compare first and third bars). To determine if ryanodine lowers the resting [Ca]_{ER} level by reducing the basal rate of ER Ca²⁺ uptake, the initial rate at which [Ca²⁺]_i rises after rapid application of the reversible SERCA inhibitor t-BuBHQ was measured before and after treatment with ryanodine (Fig. 4, D and E). Before ryanodine, t-BuBHQ elicits a transient [Ca²⁺]_i elevation that reflects Ca²⁺ release from an intracellular store; such transients

FIGURE 4. Effects of ryanodine on depolarization-induced changes in [Ca²⁺]_i and [Ca]_{ER}. (A, top traces) Comparison between [Ca²⁺]_i responses elicited by 30 mM K⁺ depolarization before (light trace) and after (dark trace) treatment with ryanodine (1 μM) to inhibit CICR. After recording a control response to 30 mM K⁺, cells were exposed to ryanodine, and then to caffeine in the presence of ryanodine, which elicited a transient [Ca²⁺]_i elevation (not shown). After washing out caffeine, all subsequent high K⁺-induced [Ca²⁺]_i responses were modified as illustrated and responsiveness to caffeine was abolished (not shown). (Bottom traces) Comparison between the upper traces and a final response elicited from the same cell after exposure to Tg (100 nM) which reversed the effect of ryanodine and speeded the rise in [Ca²⁺]_i compared with the control response. This response was elicited after the Tg-induced [Ca²⁺]_i transient was complete and resting [Ca²⁺]_i was restored (not shown). Inset shows the initial period of these responses on an expanded time scale. Cell maac53. (B) Tg-induced reversal of ryanodine's effect on [Ca²⁺]_i response kinetics does not reflect drug-induced changes in I_{Ca}; in the example shown, [Ca²⁺]_i rises more rapidly after Tg treatment even though I_{Ca} underwent considerable rundown during the period between the first and second responses. Cell ma5030. (C) Comparison between resting and depolarization-induced changes in [Ca]_{ER} in the presence and absence of ryanodine. Ryanodine reduces resting [Ca]_{ER} but enhances ER Ca accumulation during 45 s 30 mM K⁺ depolarization. (D) The reversible SERCA inhibitor t-BuBHQ (10

are not observed after treatment with Tg, arguing that Tg and t-BuBHQ deplete the same store (not shown). The abrupt rise in $[Ca^{2+}]_i$ that follows t-BuBHQ application indicates that, under resting conditions, ongoing Ca^{2+} uptake via SERCAs is balanced by passive Ca^{2+} release (Fig. 4 E, see diagrams). The initial rate of rise after SERCA inhibition provides a measure of the basal rate of release, as well as the rate of uptake that balances release under resting conditions. After treatment with ryanodine, t-BuBHQ also elicits a $[Ca^{2+}]_i$ transient (Fig. 4 D), indicating that there is still a gradient favoring passive Ca^{2+} release, but the transient is smaller and shorter in duration than the control, as expected given the lower basal $[Ca]_{ER}$. Nonetheless, the initial rate of rise is unchanged (Fig. 4, D and E; 5/5 cells), indicating that ryanodine does not alter the resting rate of Ca^{2+} uptake or release. Since ryanodine lowers resting $[Ca]_{ER}$ (and presumably the free Ca concentration within the ER, $[Ca^{2+}]_{ER}$) without altering the basal release rate, it must increase the resting ER Ca^{2+} permeability, defined as (release rate)/($[Ca^{2+}]_i - [Ca^{2+}]_{ER}$). This is the opposite of the high concentration effect of ryanodine described previously (Jones et al., 1979) but is precisely the result expected if, in addition to preventing Ca^{2+} -dependent RyR channel activation, ryanodine increases basal channel open probability.

These observations lead to the fourth important conclusion of this study. Since the ER normally accumulates Ca^{2+} when $[Ca^{2+}]_i$ is elevated during weak depolarization, and inhibition of a ryanodine-sensitive CICR pathway increases the rate of ER Ca accumulation, activation of this pathway must normally attenuate Ca^{2+} accumulation by the ER. This is an interesting mechanism, since it would involve Ca^{2+} -induced Ca^{2+} release at the level of a population of RyRs, providing a $[Ca^{2+}]_i$ -sensitive pathway for passive Ca^{2+} release from the ER that accelerates evoked $[Ca^{2+}]_i$ elevations, but in a capacity that downregulates ER Ca^{2+} accumulation.

Simulations Based on a Model of CICR Operating in a Low Gain Mode

To determine if activation of a CICR pathway could, in principle, attenuate ER Ca accumulation and accelerate depolarization-evoked $[Ca^{2+}]_i$ responses, simulations were performed based on a model of Ca^{2+} regulation (Friel, 1995) that includes two compartments representing the cytoplasm and ER containing Ca^{2+} at concentrations c_i and c_{ER} , respectively. This model assumes that Ca^{2+} is distributed uniformly within each compartment, an approximation that becomes increasingly valid as the rate of stimulated Ca^{2+} entry becomes slow enough that the rate of Ca^{2+} transport between compartments is slow compared with diffusion within compartments. Also, mitochondria are not explicitly included to facilitate analysis of the impact of a CICR pathway on net Ca^{2+} trans-

port by an intracellular pool. Although this approximation leads to results that agree with the experiment only when $[Ca^{2+}]_i$ is low and mitochondrial Ca^{2+} transport is weak, the conclusions reached below regarding the $[Ca^{2+}]_i$ dependence of net ER Ca^{2+} transport are expected to apply generally (see DISCUSSION).

In the model, Ca^{2+} extrusion across the plasma membrane is represented by an experimentally determined rate equation (Colegrove et al., 2000b; see APPENDIX), Ca^{2+} uptake by the store is controlled by a saturable pump, and the rate of passive Ca^{2+} release is the product of the total Ca^{2+} permeability of the store (P_{ER}) and a driving force ($c_i - c_{ER}$). The permeability is the sum of a constant basal component (P_{basal}) and a $[Ca^{2+}]_i$ -sensitive component (with maximal value $P_{max,RyR}$) that is intended to represent the macroscopic permeability conferred upon the store by a population of channels (e.g., RyR's) whose open probabilities increase with $[Ca^{2+}]_i$ but do not have explicit time dependence. The parameter values defining the uptake and release pathways are estimates based on our observations in sympathetic neurons (unpublished data) but the general conclusions that follow hold over a range of parameter values.

Fig. 5 A illustrates responses to Ca^{2+} entry simulated under four different conditions for comparison with experiments described above. Under control conditions (Cont), Ca^{2+} entry (Fig. 5 A, first panel) leads to a rise in c_i (second panel) that causes Ca^{2+} accumulation by the store, increasing c_{ER} from a high basal level (third panel). After suppressing Ca^{2+} uptake to represent the effects of Tg, Ca^{2+} accumulation is abolished and c_i rises more rapidly, as observed experimentally. After blocking Ca^{2+} -induced increases in permeability and raising the basal permeability of the store to model the effects of ryanodine, Ca^{2+} entry leads to a slower c_i rise but a more robust increase in c_{ER} from a lower basal level, which is also in agreement with experiments described above. Finally, after increasing the strength and c_i sensitivity of the release pathway to model the effects of caffeine (Fig. 5 A, bottom panel), c_i rises more rapidly in response to the same stimulus, and c_{ER} declines, consistent with the observed effects of caffeine on depolarization-induced $[Ca^{2+}]_i$ responses. Thus, the simple model accounts for the main observations in this study and illustrates how weak activation of a CICR pathway, operating in parallel with a Ca^{2+} uptake system, could accelerate depolarization-evoked $[Ca^{2+}]_i$ elevations by reducing the rate at which the store accumulates Ca^{2+} .

Fig. 5 B shows how the dynamics of c_i and c_{ER} change as the stimulus strength is increased when the Ca^{2+} uptake and release pathways are described as in the control case in column A. Whereas weak stimuli cause Ca^{2+} accumulation (third panel, curve 1), increasing the stimulus strength leads to progressively weaker accumulation (Fig. 5 B second and third

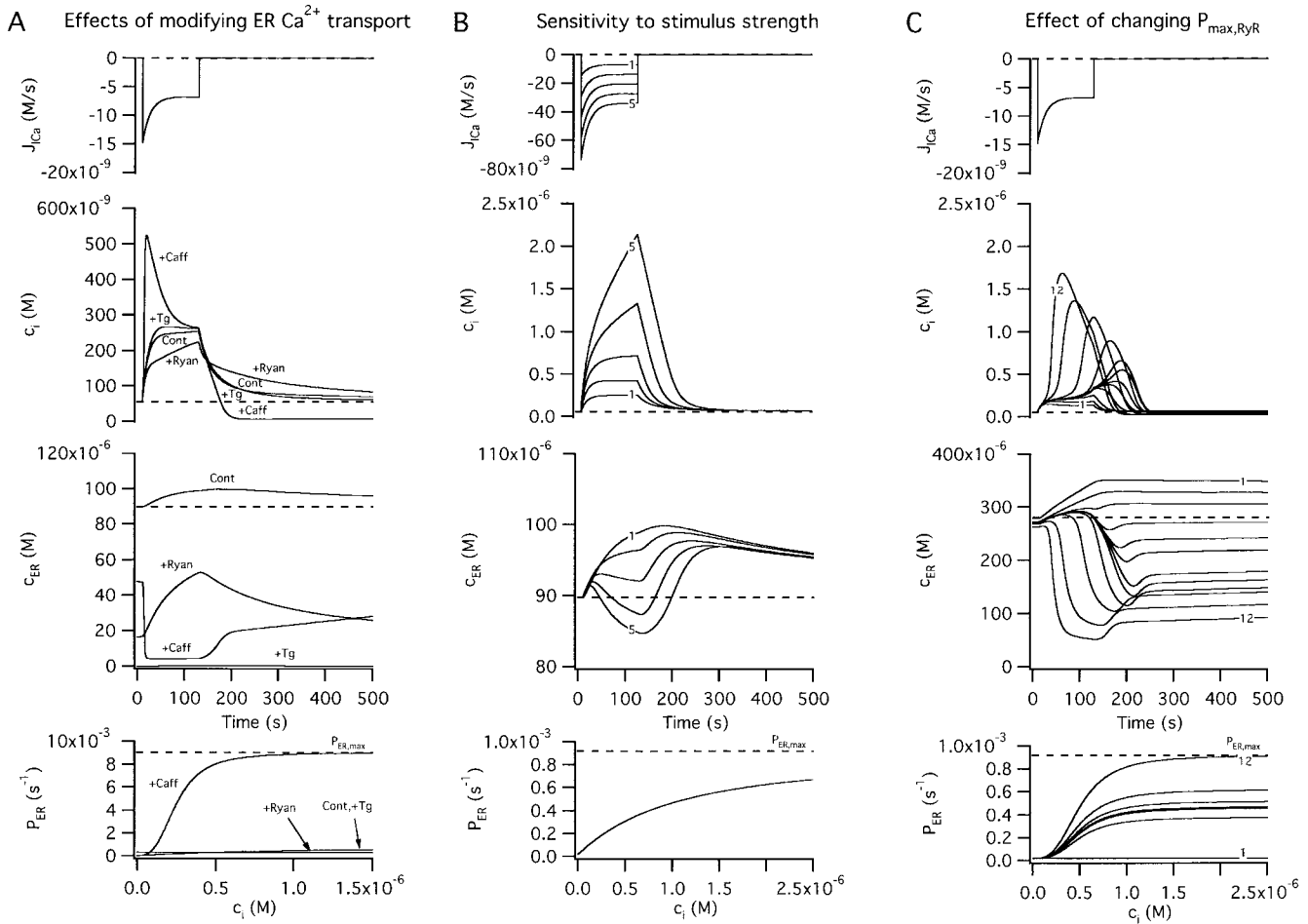


FIGURE 5. Simulated changes in c_i and c_{ER} induced by Ca²⁺ entry. A–C illustrate simulated effects of Ca²⁺ entry (top row) on the concentrations of cytosolic Ca²⁺ (c_i , second row) and intraluminal Ca²⁺ (c_{ER} , third row); bottom row shows how the total Ca²⁺ permeability of the internal pool depends on c_i . Components of the net Ca²⁺ flux across the plasma membrane (J_{Ca} , J_{extru}) and of the net ER Ca²⁺ flux (J_{SERCA} , $J_{release}$) are defined in the APPENDIX and illustrated in Fig. 7. (A) Simulated responses under four conditions that can be compared with results described in this study. Under control conditions (Cont), Ca²⁺ entry increases c_i but at a rate that is attenuated by Ca²⁺ accumulation, which causes c_{ER} to rise from a high basal level. After inhibiting the uptake pathway (+Tg), c_{ER} remains low and c_i increases more rapidly during stimulation than in the control. After inhibiting CICR and increasing P_{basal} to model the effects of ryanodine (+Ryan), c_i rises more slowly and c_{ER} rises more rapidly from a lower resting level. Finally, after increasing the maximal rate of CICR and its c_i sensitivity (+Caff), the rise in c_i triggers net Ca²⁺ release so that c_{ER} declines and the c_i rise is accelerated, leading to a transient c_i overshoot. For the control response, $k_{leak} = 1.5 \times 10^{-7} \text{ s}^{-1}$, $c_o = 2 \text{ mM}$, $V_{max,extru} = 25 \text{ nM/s}$, $EC_{50,extru} = 386 \text{ nM}$, $n_{extru} = 2.4$, $V_{max,SERCA} = 70 \text{ nM/s}$, $EC_{50,SERCA} = 700 \text{ nM}$, $n_{SERCA} = 1$, $P_{basal} = 1.78 \times 10^{-5} \text{ s}^{-1}$, $P_{max,RyR} = 9 \times 10^{-4} \text{ s}^{-1}$, $EC_{50,RyR} = 1 \text{ }\mu\text{M}$, $n_{RyR} = 1$ and $\gamma_{ER} = 0.01$. To simulate responses after treatment with Tg, $V_{max,SERCA}$ was set to zero while all other parameters had their control values. To simulate responses in the presence of ryanodine, $P_{max,RyR}$ was set to zero and P_{basal} was increased to $3 \times 10^{-4} \text{ s}^{-1}$. To simulate the effects of caffeine, $P_{max,RyR}$ was increased to $9 \times 10^{-3} \text{ s}^{-1}$, $EC_{50,RyR}$ was reduced to 250 nM, and n_{RyR} was increased to 3. Ca²⁺ entry was represented by fitting a triple exponential function to a representative J_{Ca} measurement obtained during a 40 s depolarization and extrapolating in time; tail currents were not included. (B) Simulated responses elicited by stimuli of increasing strength (curves 1–5) using control parameters from A. (C) Simulated responses to a fixed stimulus illustrating the effect of increasing the c_i -sensitive permeability, $P_{max,RyR}$ (curves 1–12) with $EC_{50,RyR} = 500 \text{ nM}$ and $n_{RyR} = 3$. The effect of these changes on total permeability (P_{ER}) is shown at bottom.

curves), until the balance between uptake and release tips in favor of net Ca²⁺ release (Fig. 5 B, curves 4–5). The accompanying study demonstrates such a transition in sympathetic neurons. Fig. 5 C illustrates a similar transition that results from increasing the maximal c_i -sensitive permeability of the store ($P_{max,RyR}$) in the case where the stimulus is fixed and the c_i dependence of the permeability is steep. When $P_{max,RyR}$ is

small (Fig. 5 C, bottom panel), the store is a Ca²⁺-regulated buffer (Fig. 5 C, second and third panels), but if this parameter is increased sufficiently, the same stimulus triggers net Ca²⁺ release (e.g., see curve 12). In the DISCUSSION, we will show how such quantitative properties of the CICR pathway are expected to contribute to qualitative properties of cellular Ca²⁺ regulation.

Returning to the main goal of the present study, we propose that small $[Ca^{2+}]_i$ elevations elicited by weak depolarization increase the rate of passive Ca^{2+} release via a Ca^{2+} - and ryanodine-sensitive CICR pathway, but because release is slower than uptake, the overall effect is to reduce the rate of ER Ca^{2+} accumulation. In terms of the ideas presented earlier, such a low gain mode of CICR would reduce the outward flux J_{Σ} during depolarization and shift the total cytosolic Ca^{2+} flux during stimulation ($J_{Ca} + J_{\Sigma}$) toward more negative values, leading to a faster rise in $[Ca^{2+}]_i$ than would be expected without CICR. In this mode, activation of CICR accelerates the rise in $[Ca^{2+}]_i$ elicited by Ca^{2+} entry, but does so by reducing the strength of ER Ca^{2+} buffering.

DISCUSSION

Our results show that small $[Ca^{2+}]_i$ elevations evoked by weak depolarization lead to Ca^{2+} accumulation by the ER, and that Ca^{2+} accumulation becomes stronger after inhibiting CICR with ryanodine. The companion article (see Hongpaisan et al., 2001, in this issue) shows that as stimulus-evoked $[Ca^{2+}]_i$ elevations become larger, ER Ca^{2+} accumulation becomes progressively weaker, and that at high $[Ca^{2+}]_i$, the ER becomes a Ca^{2+} source. Our results suggest a simple explanation: progressive activation of a $[Ca^{2+}]_i$ -sensitive CICR pathway that operates in parallel with SERCA pumps to regulate net ER Ca^{2+} transport.

Comparison with Previous Studies

Studies in many neuronal cell types have identified a Ca^{2+} store that expresses functional RyRs and can be discharged by caffeine (Kuba, 1994; Usachev and Thayer, 1999). This and the companion article (see Hongpaisan et al., 2001, in this issue) provide direct confirmation that this Ca^{2+} store is the ER, contributing to the already large body of evidence that this organelle is important in cellular Ca^{2+} regulation (Meldolesi and Pozzan, 1998). Although contributions from caffeine-modified RyRs to depolarization-evoked $[Ca^{2+}]_i$ signals have been clear, it has not been obvious how RyRs participate in calcium signaling in the absence of CICR modifiers. In sympathetic neurons, the observation that ryanodine slows depolarization-evoked $[Ca^{2+}]_i$ elevations raised the possibility that activation of a CICR pathway amplifies the effect of Ca^{2+} entry on $[Ca^{2+}]_i$ (Friel and Tsien, 1992a). This was supported by work of Hua et al. (1993) showing that depolarization-induced $[Ca^{2+}]_i$ elevations increase supralinearly with Ca^{2+} load and exhibit a form of paired-pulse facilitation. Similar observations have been made in other cells (Shmigol et al., 1995; Llano et al., 1994). Although these results are consistent with Ca^{2+} -induced net Ca^{2+} release from an intracellular Ca^{2+} store, they

are also consistent with $[Ca^{2+}]_i$ -dependent attenuation of intracellular Ca^{2+} buffering or sequestration. One approach to distinguishing between these possibilities is based on the use of CICR inhibitors like ryanodine. However, our results show that specific inhibition of CICR is expected to slow depolarization-evoked $[Ca^{2+}]_i$ responses irrespective of the direction of net ER Ca^{2+} transport. Therefore, additional information is required. Several studies have provided examples where Ca^{2+} entry triggers net CICR (Cohen et al., 1997; Alonso et al., 1999; Emptage et al., 1999; Sandler and Barbara, 1999). However, to our knowledge, the present study is the first to show that activation of a Ca^{2+} - and ryanodine-sensitive Ca^{2+} release process during periods of Ca^{2+} entry accelerates $[Ca^{2+}]_i$ responses by attenuating ER Ca accumulation.

Impact of CICR on Net ER Ca^{2+} Transport

At each instant in time during stimulation, the rate of net ER Ca^{2+} transport should depend on the relative rates of Ca^{2+} uptake via SERCA pumps and passive Ca^{2+} release via RyRs, D-myoinositol 1,4,5-trisphosphate ($InsP_3$) receptors (Pfaffinger et al., 1988), and possibly other uncharacterized Ca^{2+} transport pathways. The finding that weak depolarization leads to ER Ca accumulation indicates that small $[Ca^{2+}]_i$ elevations stimulate Ca^{2+} uptake more strongly than release. Stimulated Ca^{2+} uptake is expected since SERCA activity increases with $[Ca^{2+}]_i$ (Lytton et al., 1992), but how would the rate of Ca^{2+} release be expected to change in response to a rise in $[Ca^{2+}]_i$? This rate should depend on the driving force for passive Ca^{2+} movement between the ER and cytoplasm ($\sim [Ca^{2+}]_i - [Ca^{2+}]_{ER}$) and the Ca^{2+} permeability of the ER (P_{ER}). If P_{ER} were constant, a rapid rise in $[Ca^{2+}]_i$ (rapid enough so that $[Ca^{2+}]_{ER}$ does not change very much) would reduce the driving force and lower the rate of release. If P_{ER} increased weakly with $[Ca^{2+}]_i$ (e.g., as a result of $[Ca^{2+}]_i$ -dependent RyR activation), the effect of reduced driving force on release rate would be partially overcome; if P_{ER} increased more steeply with $[Ca^{2+}]_i$, the rate of release could rise. Our results are consistent with a Ca^{2+} -induced increase in the rate of passive Ca^{2+} release that is smaller than the stimulated increase in uptake rate. In this case, Ca^{2+} accumulation would occur as $[Ca^{2+}]_i$ rises but at a reduced rate because of RyR activation that, in effect, short circuits the uptake process and permits $[Ca^{2+}]_i$ to rise more rapidly during periods of Ca^{2+} entry. Inhibition of the permeability increase (e.g., with ryanodine) would prevent the increase in release rate, augment the imbalance between uptake and release, and strengthen Ca accumulation, causing $[Ca^{2+}]_i$ to rise more slowly during stimulation.

Effects of Ryanodine on Net ER Ca^{2+} Transport

Slowing of depolarization-evoked $[\text{Ca}^{2+}]_i$ responses by ryanodine has been interpreted to mean that Ca^{2+} entry normally triggers net Ca^{2+} release. This conclusion is based on the assumption, previously untested, that ryanodine renders the ER so leaky that active Ca^{2+} accumulation becomes impossible. However, if ryanodine only modestly increases ER Ca^{2+} permeability, its effects on evoked $[\text{Ca}^{2+}]_i$ responses are consistent with either triggered net Ca^{2+} release or attenuated Ca^{2+} accumulation. We found that ryanodine (1 μM): abolishes caffeine responsiveness; reduces basal $[\text{Ca}]_{\text{ER}}$ (and presumably $[\text{Ca}^{2+}]_{\text{ER}}$, although this was not measured directly); and enhances depolarization-induced ER Ca accumulation. Each effect follows from known actions of ryanodine on RyRs (see MATERIALS AND METHODS). Inhibition of caffeine responsiveness is expected based on reduced RyR sensitivity to Ca^{2+} , and a reduction in basal $[\text{Ca}]_{\text{ER}}$ follows from increased channel open probability. The finding that ryanodine does not alter the basal rate of Ca^{2+} release argues that once RyRs are modified, $[\text{Ca}^{2+}]_{\text{ER}}$ falls until a new steady-state level is reached where Ca^{2+} release once again balances Ca^{2+} uptake. In principle, either action of ryanodine could contribute to inhibition of caffeine-induced Ca^{2+} release. However, since net Ca^{2+} release can be stimulated by SERCA inhibition after ryanodine treatment, loss of caffeine responsiveness cannot be accounted for entirely by depletion of the ER, and is more likely a result of reduced RyR sensitivity to Ca^{2+} . We propose that Ca^{2+} accumulation by the ER is enhanced in ryanodine-treated cells because as $[\text{Ca}^{2+}]_i$ rises during stimulation, the rate of passive Ca^{2+} release falls, in contrast to the rise that occurs in untreated cells. This would increase the imbalance between ER Ca^{2+} uptake and release rates, favoring stronger Ca accumulation.

Clearly, other factors could contribute to our observations. For example, after ryanodine treatment, the reduction in basal $[\text{Ca}]_{\text{ER}}$ could cause the ER to become a less saturated, and therefore more powerful, Ca^{2+} buffer. Although our data do not address this point directly, it should be mentioned that this explanation cannot account for net Ca^{2+} release at high $[\text{Ca}^{2+}]_i$. In contrast, graded activation of a CICR pathway provides a parsimonious explanation for attenuated Ca accumulation at low $[\text{Ca}^{2+}]_i$, net Ca^{2+} release at high $[\text{Ca}^{2+}]_i$ (Hongpaisan et al., 2001), and stronger ER Ca^{2+} buffering after ryanodine treatment, without making any assumptions about the properties of intraluminal Ca^{2+} buffers. Furthermore, simulations in Fig. 5 show that this idea is reasonable and can account for our general observations.

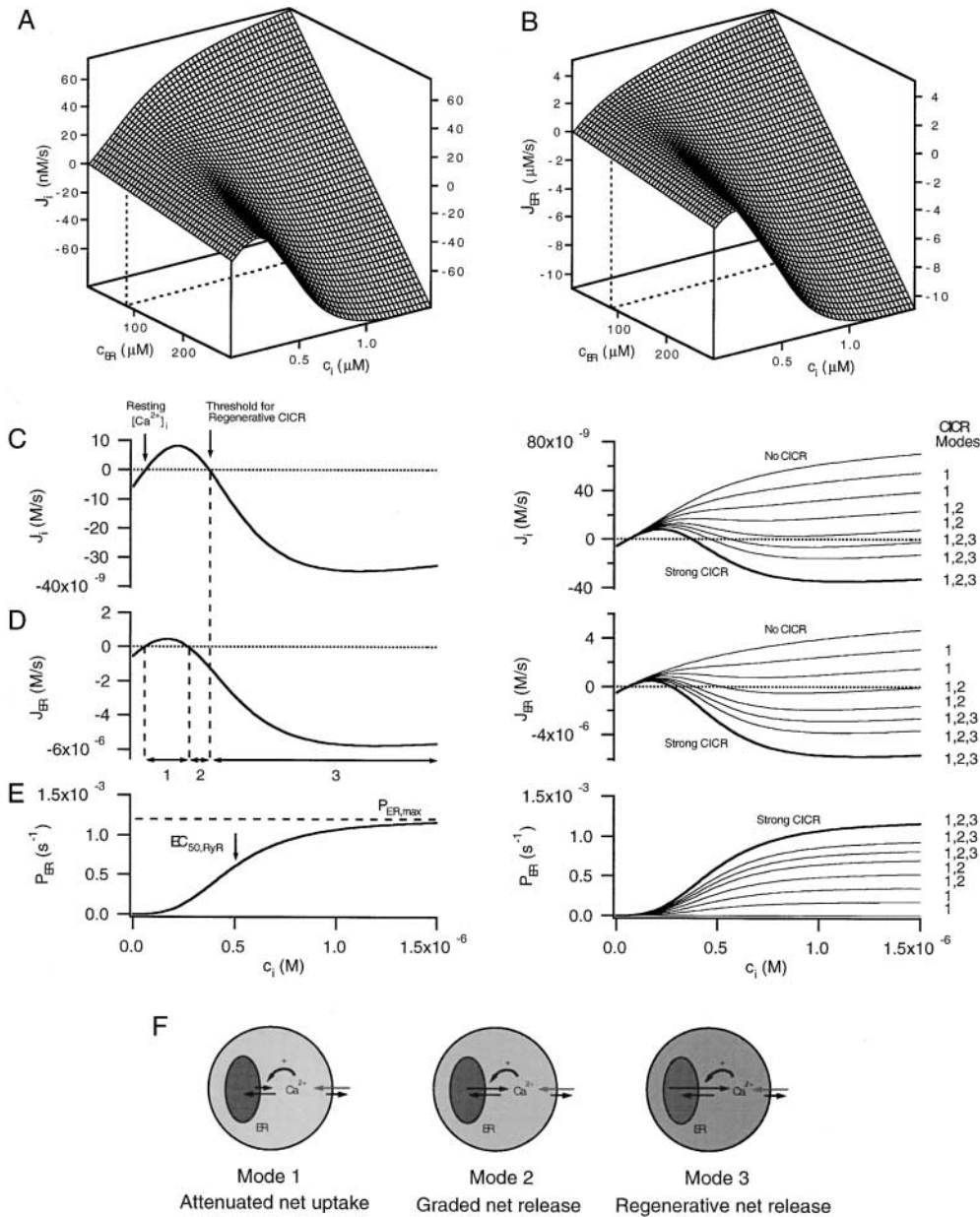
The findings described in this study are consistent with a single ER Ca^{2+} pool expressing multiple transport pathways (SERCAs, RyRs, InsP_3 s, etc.), but it must

be asked if they can also be explained by structurally distinct ryanodine-sensitive and -insensitive pools that are both sensitive to Tg and, respectively, release and take up net Ca^{2+} during depolarization. Although the existence of such pools cannot be excluded, our measurements do not detect them (see companion article, Hongpaisan et al., 2001, in this issue). Moreover, the observation that ryanodine does not change the basal rate of Ca^{2+} uptake (Fig. 4, D and E) severely limits such multipool models. If the ER did consist of two (or more) distinct pools, the basal rate of Ca^{2+} uptake would be the sum of the rates of uptake by the individual pools. If ryanodine specifically eliminated contributions from the ryanodine-sensitive pool by rendering it so leaky that Ca^{2+} becomes passively distributed between the ER and cytoplasm, then it would also reduce the initial rate at which $[\text{Ca}^{2+}]_i$ rises after exposure to t-BuBHQ, but no such change was observed. Insensitivity of the initial rate to ryanodine would require that the resting rate of Ca^{2+} uptake by the ryanodine-sensitive pool be undetectably low, which is difficult to reconcile with the observation that caffeine-induced $[\text{Ca}^{2+}]_i$ transients are larger if they are preceded by brief depolarizations that raise $[\text{Ca}^{2+}]_i$ to levels comparable to those shown in this study to stimulate ER Ca^{2+} accumulation (unpublished data). The single-pool model, on the other hand, provides a simple explanation of the results. A similar conclusion was reached by Khodakhah and Armstrong (1997) from their studies of cerebellar Purkinje neurons.

Qualitative Properties of CICR: Dual Regulation of Cytoplasmic and ER Calcium Levels

Our results indicate that CICR modulates ER Ca^{2+} accumulation during weak stimulation, but they do not preclude net Ca^{2+} release via CICR at higher $[\text{Ca}^{2+}]_i$. Indeed, as illustrated in Fig. 5 B, theory suggests that under certain conditions, larger stimulus-evoked $[\text{Ca}^{2+}]_i$ elevations can lead to a transition from regulated Ca^{2+} buffering to triggered net Ca^{2+} release, and the model provides a framework for evaluating the conditions under which such a transition can occur. Since mitochondria are not included in the model, simulations can only be compared directly to results obtained under conditions where mitochondrial Ca^{2+} transport is weak. However, Ca^{2+} transport by mitochondria is not expected to influence the $[\text{Ca}^{2+}]_i$ dependence of net ER Ca^{2+} transport, per se, but rather the range over which $[\text{Ca}^{2+}]_i$ varies during stimulation (see companion article, Hongpaisan et al., 2001, in this issue). Therefore, analysis of the case without mitochondria should provide insight into the properties of ER Ca^{2+} transport even when mitochondrial Ca^{2+} transport is appreciable.

According to the model, c_i and c_{ER} dynamics depend on the total cytosolic Ca^{2+} flux (J_i) and the net ER Ca^{2+}



$P_{max,RyR}$ were ($10^{-4} s^{-1}$) as follows: 0, 1.8, 3.6, 5.4, 7.2, 8.4, 9.6, and 12. (F) Relationship between the rates of Ca^{2+} uptake, release, and extrusion in each CICR mode. Relative free Ca concentrations are represented by shading (darker = higher $[Ca^{2+}]$). In Mode 1 (low c_i), uptake is faster than release, whereas in Mode 2 (intermediate c_i), release is faster than uptake, causing net release but at a slower rate than extrusion. In Mode 3 CICR (high c_i), net release is faster than extrusion, leading to positive feedback and a regenerative rise in c_i . Surface in A describes the total Ca^{2+} flux representing uptake, release, and extrusion (dark arrow on the plasma membrane in F) in the absence of stimulated Ca^{2+} entry. During stimulated Ca^{2+} entry (light arrows on the plasma membrane), the surface in A would be displaced downward by an amount J_{ICa} , which depends on time.

flux (J_{ER}), respectively, which in turn display the combined $[Ca^{2+}]$ dependencies of the underlying transporters. Fig. 6 (A and B) shows how these fluxes depend on c_i and c_{ER} when $J_{ICa} = 0$ in a particular case where the Ca^{2+} permeability of the store increases steeply with c_i (Hill coefficient 3) and becomes large when c_i is high because the c_i -sensitive permeability ($P_{max,RyR}$) is large (Fig. 6 E, left). Slices from the surfaces in Fig. 6 (A and B, dashed lines) show how J_i and J_{ER} change with c_i at

constant c_{ER} (Fig. 6, C and D, left), in particular, giving the instantaneous rates at which c_i and c_{ER} would change if c_i were raised rapidly by a very brief stimulus without perturbing c_{ER} . These curves are analogous to the momentary current-voltage relations described by Jack et al. (1983). As with membrane potential dynamics, c_i and c_{ER} dynamics depend on the stimulus protocol: two stimuli that raise c_i to the same steady-state level but at different rates could have very different effects on

FIGURE 6. Three modes of net CICR. (A and B) Surfaces showing how the net cytoplasmic and ER Ca^{2+} fluxes, J_i and J_{ER} , depend on c_i and c_{ER} in the case $J_{ICa} = 0$ according to the model described in the APPENDIX. Slices from these surfaces at constant c_{ER} (dashed lines) illustrate the nonlinear c_i dependencies of the underlying Ca^{2+} fluxes, whereas curves at constant c_i illustrate the linear c_{ER} dependence of the fluxes. Parameters describing the c_i -sensitive permeability are as follows: $P_{max,RyR} = 1.2 \times 10^{-3} s^{-1}$, $EC_{50,RyR} = 500$ nM, $n_{RyR} = 3$. Basal $c_{ER} = 90.8$ μ M. (C and D, left) Slices from the surfaces in A and B at constant c_{ER} . These flux/ c_i relations illustrate the basis for three qualitatively distinct modes of net CICR: Mode 1 ($J_i > 0$, $J_{ER} > 0$), Mode 2 ($J_i > 0$, $J_{ER} < 0$), and Mode 3 ($J_i < 0$, $J_{ER} < 0$). The ranges of c_i in which these modes occur are indicated in D (bottom). (E, left) c_i dependence of the Ca^{2+} permeability, P_{ER} . (C and D, right) Slices from different J_i and J_{ER} surfaces with different values of $P_{max,RyR}$ show that as this parameter is increased from zero (no CICR) to a large value (strong CICR) additional modes of net CICR become available. Bold traces represent the same curves shown at left but on a different ordinate scale. In each case, c_{ER} was fixed at its resting value, which depended on $P_{max,RyR}$. Values of

c_i and c_{ER} dynamics owing to differences in c_{ER} that arise during stimulation. Nevertheless, at each instant in time, the net fluxes J_i and J_{ER} would be defined by the magnitudes of c_i , c_{ER} and J_{iCa} at that time.

In the case illustrated, J_i first increases with c_i and crosses the zero net flux axis at a (stable) steady-state value (Fig. 6 C, left arrow) that is well below the Ca^{2+} concentration ($EC_{50,RyR}$) where the c_i -sensitive permeability is half maximally activated (Fig. 6 E, left). However, when c_i is higher, the permeability of the store is larger, causing J_i to turn downward, cross the zero flux axis with negative slope at an (unstable) steady-state (panel C, right arrow), and then become negative. There are three ranges of c_i in which J_i and J_{ER} show distinct c_i -dependencies, revealing three modes of CICR (Fig. 6 D, arrows 1–3; Friel, 1998). When c_i is above the resting level, but low compared with $EC_{50,RyR}$, J_i and J_{ER} are both positive (Mode 1 CICR). J_{ER} is positive because passive Ca^{2+} release is slower than Ca^{2+} uptake, causing the store to act as a buffer. In this case, activation of the c_i -sensitive permeability during stimulation lowers the rate of Ca^{2+} accumulation by the store and accelerates evoked increases in c_i . Over the intermediate c_i range, J_i is positive and J_{ER} is negative (Mode 2 CICR). J_{ER} becomes negative when passive Ca^{2+} release is faster than uptake, leading to net release, which further increases the rate at which c_i rises in response to stimulated Ca^{2+} entry, and causes c_{ER} to decline. Finally, at higher c_i , both J_i and J_{ER} become inward fluxes (Mode 3 CICR). A brief stimulus that brings c_i within this range would stimulate Ca^{2+} release at such a high rate that it overwhelms Ca^{2+} extrusion, leading to a regenerative rise in c_i and fall in c_{ER} . The zero crossing in this case represents the threshold for regenerative net CICR (Fig. 6C, see right arrow). When c_i is very high compared with $EC_{50,RyR}$, J_i once again increases monotonically with c_i , representing the case where the total Ca^{2+} permeability is high and essentially constant (not shown).

With fixed rate characteristics for Ca^{2+} extrusion and uptake, the quantitative properties of the c_i -dependent permeability determine which modes of net CICR can be expressed. Fig. 6 (C and D, right) shows families of slices from J_i and J_{ER} surfaces like those in Fig. 6 (A and B) at constant c_{ER} but with different values of $P_{max,RyR}$ (Fig. 6 E, right). $P_{max,RyR}$ would depend on the number of Ca^{2+} release channels, their maximal open probability at high c_i , and unitary Ca^{2+} permeability. When $P_{max,RyR}$ is small, only Mode 1 CICR is available, irrespective of the stimulus strength. This would describe a cell in which Ca^{2+} release channels are present at low density compared with SERCA pumps. With intermediate values of $P_{max,RyR}$, both Modes 1 and 2 are available, but not Mode 3, which could represent a cell in which RyR density relative to SERCA pumps is somewhat higher, but plasma membrane Ca^{2+} extrusion systems

are powerful. Finally, when $P_{max,RyR}$ is large, all three modes are available, which includes the possibility of regenerative Ca^{2+} release if c_i is raised beyond the appropriate threshold. For example, this could represent a case in which RyRs are expressed at high density compared with SERCAs or are modified pharmacologically so that their maximal open probability is high. Cells having different levels of channel expression would be described by different values of $P_{max,RyR}$, as would a given cell type before and after a pharmacological modification (e.g., by caffeine). Naturally occurring variations in the density or unitary properties of RyRs or SERCAs could contribute to variability of response properties observed in different populations of sympathetic neurons (Cseresnyes et al., 1999) or different types of cells. These general conclusions are not limited to RyR-mediated CICR and apply equally well to $InsP_3$ receptor mediated CICR.

Which modes of CICR are expressed by sympathetic neurons? Results from the present study demonstrate Mode 1 CICR, and results in the companion article (see Hongpaisan et al., 2001, in this issue) show that when $[Ca^{2+}]_i$ is raised to higher levels by stronger depolarizing stimuli, Mode 2 or 3 CICR can occur. Regenerative depolarization-induced $[Ca^{2+}]_i$ elevations have been reported in sympathetic neurons in the absence of caffeine (Lipscombe et al., 1988; Hua et al., 1993), further pointing to the possibility of Mode 3 CICR. Regenerative $[Ca^{2+}]_i$ increases can be elicited in the presence of caffeine in these and other cells (Friel and Tsien, 1992b; Usachev and Thayer, 1997), clearly demonstrating Mode 3 CICR under these conditions.

Implications for Calcium Signaling

Activation of a CICR pathway is expected to have direct effects on stimulus-induced changes in $[Ca^{2+}]_i$ within the cytoplasm and the ER, as well as indirect effects on other organelles that exchange Ca^{2+} with the cytoplasmic pool. Modulation of depolarization-evoked changes in $[Ca^{2+}]_i$ by CICR may well contribute to the control of membrane excitability and neurotransmitter release (Narita et al., 1998, 2000; Llano et al., 2000) in a way that is sensitive to stimulus history. Our results indicate that weak and strong depolarizing stimuli, while evoking graded increases in $[Ca^{2+}]_i$, could have opposite effects on $[Ca^{2+}]_{ER}$, leading to qualitatively different patterns of activity among Ca^{2+} -sensitive effectors within the cytosol and the ER (Corbett and Michalak, 2000). Weak activation of a CICR pathway would provide a mechanism for increasing the impact of Ca^{2+} entry on $[Ca^{2+}]_i$ without reducing $[Ca]_{ER}$. In this regard, it is interesting to note that reducing $[Ca]_{ER}$ has been shown in some cells to be proapoptotic (Wei et al., 1998). Finally, it is expected that the expression levels of Ca^{2+} transporters, as well as their state of modula-

tion, define which modes of CICR can occur. This may play a role in defining differences between cells from different tissues, species and developmental stages, as well as adaptive changes that occur after perturbations of Ca^{2+} delivery in disease (Dove et al., 2000).

A Note on Terminology

Our results underscore a basic ambiguity in the phrase “ Ca^{2+} -induced Ca^{2+} release” that arises because there is a distinction between Ca^{2+} transport via a CICR pathway, and net Ca^{2+} transport by the ER. CICR is usually used to refer to net Ca^{2+} release, but the results presented here indicate that activation of a Ca^{2+} -sensitive release pathway can regulate ER Ca^{2+} accumulation. In both cases, activation of the CICR pathway accelerates depolarization-evoked $[\text{Ca}^{2+}]_i$ elevations, but, in one case, $[\text{Ca}]_{\text{ER}}$ rises whereas in the other it falls. In principle, CICR could refer to either situation, describing passive release via a Ca^{2+} -sensitive permeability without reference to the direction of net organellar Ca^{2+} movement, or Ca^{2+} -induced net Ca^{2+} release. Since the second definition necessarily involves the relationship between a CICR pathway and other transport systems, we prefer the first definition, and use the phrase “net CICR” to refer to the second. According to this usage, CICR refers to a passive macroscopic Ca^{2+} flux whose impact on intraluminal Ca^{2+} levels is context-dependent.

APPENDIX

Description of the Model

The dynamics of the free Ca^{2+} concentration within the cytosol (c_i) and the ER (c_{ER}) were represented by the following differential equations (Eqs. 1 and 2; see Fig. 7).

$$\frac{dc_i}{dt} = -J_i \quad (1)$$

$$\frac{dc_{\text{ER}}}{dt} = \frac{J_{\text{ER}}}{\gamma_{\text{ER}}} \quad (2)$$

where

$$J_i = J_{\text{pm}} + J_{\text{ER}} \quad (3)$$

and the intercompartmental fluxes J_{pm} and J_{ER} depend on the relative rates of transport via different pathways as follows:

$$J_{\text{pm}} = J_{\text{extru}} + J_{\text{ICa}} \quad (4)$$

$$J_{\text{ER}} = J_{\text{SERCA}} + J_{\text{Release}} \quad (5)$$

where

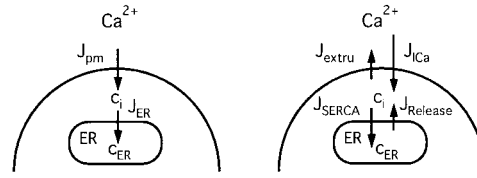


FIGURE 7. Schematic of the model. (left) Model includes two compartments representing the cytoplasm and ER with Ca^{2+} concentrations c_i and c_{ER} . The extracellular Ca^{2+} concentration is assumed to be constant. c_i and c_{ER} change under the influence of the intercompartmental net Ca^{2+} fluxes J_{pm} and J_{ER} . (right) Components of the intercompartmental Ca^{2+} fluxes. J_{pm} is the sum of the rates of Ca^{2+} entry through voltage-gated Ca^{2+} channels (J_{ICa}) and Ca^{2+} extrusion (J_{extru}). J_{ER} is the sum of the rates of Ca^{2+} uptake (J_{SERCA}) and passive Ca^{2+} release (J_{Release}). See APPENDIX for definitions of the fluxes and their c_i and c_{ER} dependencies and figure legends for parameter values.

$$J_{\text{extru}} = k_{\text{leak}}(c_i - c_o) + \frac{V_{\text{max,extru}}}{1 + \left(\frac{\text{EC}_{50,\text{extru}}}{c_i}\right)^{n_{\text{extru}}}} \quad (6)$$

$$J_{\text{ICa}} = \frac{I_{\text{Ca}}}{2Fv_i\kappa_i^T} \quad (7)$$

$$J_{\text{SERCA}} = \frac{V_{\text{max,SERCA}}}{1 + \left(\frac{\text{EC}_{50,\text{SERCA}}}{c_i}\right)^{n_{\text{SERCA}}}} \quad (8)$$

$$J_{\text{Release}} = P_{\text{ER}}(c_i - c_{\text{ER}}) \quad (9)$$

and

$$P_{\text{ER}} = P_{\text{basal}} + \frac{P_{\text{max,RyR}}}{1 + \left(\frac{\text{EC}_{50,\text{RyR}}}{c_i}\right)^{n_{\text{RyR}}}} \quad (10)$$

$$\gamma_{\text{ER}} = \frac{v_{\text{ER}}\kappa_{\text{ER}}^T}{v_i\kappa_i^T} \quad (11)$$

k_{leak} , c_o , $V_{\text{max,extru}}$, $\text{EC}_{50,\text{extru}}$, n_{extru} , F , $V_{\text{max,SERCA}}$, $\text{EC}_{50,\text{SERCA}}$, n_{SERCA} , P_{basal} , $P_{\text{max,RyR}}$, $\text{EC}_{50,\text{RyR}}$, n_{RyR} , and γ_{ER} are constants. c_o is the extracellular Ca^{2+} concentration and F is the Faraday constant.

Eqs. 3–9 describe the rate of total Ca^{2+} transport by the respective pathways divided by the cytoplasmic volume (v_i) and a buffering factor that is the ratio of changes in total cytoplasmic Ca concentration that accompany small changes in free Ca concentration (κ_i^T , Colegrove et al., 2000a,b). Fluxes that raise c_i are negative and fluxes that lower c_i are positive. J_{extru} is the sum of plasma membrane pump and leak fluxes. P_{ER} describes the total Ca^{2+} permeability of the ER store and consists of a constant basal component (P_{basal}) and a c_i -dependent component that increases saturably with c_i (half-maximal activation when $c_i = \text{EC}_{50,\text{RyR}}$) and approaches $P_{\text{max,RyR}}$ when is high c_i (Fig. 5, A–C, bottom).

In the model, the c_i dependence of P_{ER} is responsible for CICR. Estimation of parameters for Eq. 6 is described in Colegrove et al. (2000b), measurement of κ_i^T is described in MATERIALS AND METHODS, and parameters for Eqs. 8–11 are estimates based on our unpublished data.

The authors thank Drs. S.W. Jones, D. Kunze and J. Ma for their helpful comments on the manuscript.

This work was supported by a grant (No. NS-33514) from the NIH and by the NIH Intramural Research Program.

REFERENCES

- Albrecht, M.A., and D.D. Friel. 1997. Ryanodine-induced enhancement of Ca^{2+} sequestration by intracellular stores in sympathetic neurons. *Biophys. J.* 72:298 (Abstr.).
- Alonso, M.T., M.J. Barrero, P. Michelena, E. Carnicero, I. Cuchillo, A.G. Garcia, J. Garcia-Sancho, M. Montero, and J. Alvarez. 1999. Ca^{2+} -induced Ca^{2+} release in chromaffin cells seen from inside the ER with targeted aequorin. *J. Cell Biol.* 144:214–254.
- Babcock, D.F., and B. Hille. 1998. Mitochondrial oversight of cellular Ca^{2+} signaling. *Curr. Opin. Neurobiol.* 8:398–404.
- Berridge, M.J. 1998. Neuronal calcium signaling. *Neuron.* 21:13–26.
- Berridge, M.J., T.R. Cheek, D.L. Bennett, and M.D. Bootman. 1995. Ryanodine Receptors and intracellular calcium signaling. In *Ryanodine receptors*. V. Sorrentino, editor. CRC Press, Boca Raton, 119–153.
- Boyce, W.E., and R.C. DiPrima. 1969. *Elementary Differential Equations*. John Wiley and Sons, Inc. New York. 353–357.
- Chen, S.R.W., P. Li, and L. Zhang. 2001. Sensitization of the Ca^{2+} release channel (ryanodine receptor) to Ca^{2+} activation by ryanodine. *Biophys. J.* 80:384 (Abstr.).
- Cohen, A.S., K.A. Moore, R. Bangalore, M.S. Jafri, D. Weinreich, and J.P.Y. Kao. 1997. Ca^{2+} -induced Ca^{2+} release mediates Ca^{2+} transients evoked by single action potentials in rabbit vagal afferent neurones. *J. Physiol.* 499:315–328.
- Colegrove, S.L., M.A. Albrecht, and D.D. Friel. 2000a. Dissection of mitochondrial Ca^{2+} uptake and release fluxes after depolarization-evoked $[Ca^{2+}]_i$ elevations in sympathetic neurons. *J. Gen. Physiol.* 115:351–370.
- Colegrove, S.L., M.A. Albrecht, and D.D. Friel. 2000b. Quantitative analysis of mitochondrial Ca^{2+} uptake and release pathways in sympathetic neurons: reconstruction of the recovery after depolarization-evoked $[Ca^{2+}]_i$ elevations. *J. Gen. Physiol.* 115:371–388.
- Corbett, E.F., and M. Michalak. 2000. Calcium, a signaling molecule in the endoplasmic reticulum? *Trends Biochem. Sci.* 25:307–311.
- Coronado, R., J. Morrissette, M. Sukhareva, and D.M. Vaughan. 1994. Structure and function of ryanodine receptors. *Am. J. Physiol.* 266:C1485–C1504.
- Cseresnyes, Z., A.I. Bustamante, and M.F. Schneider. 1999. Caffeine-induced $[Ca^{2+}]_i$ oscillations in neurones of frog sympathetic ganglia. *J. Physiol.* 514:83–99.
- Dove, L.S., S.S. Nahm, D. Murchison, L.C. Abbott, and W.H. Griffith. 2000. Altered calcium homeostasis in cerebellar Purkinje cells of leaner mutant mice. *J. Neurophysiol.* 84:513–524.
- Emptage, N., T.V. Bliss, and A. Fine. 1999. Single synaptic events evoke NMDA receptor-mediated release of calcium from internal stores in hippocampal dendritic spines. *Neuron.* 22:115–124.
- Friel, D.D. 1995. $[Ca^{2+}]_i$ oscillations in sympathetic neurons: an experimental test of a theoretical model. *Biophys. J.* 68:1752–1766.
- Friel, D.D., and R.W. Tsien. 1992a. A caffeine- and ryanodine-sensitive Ca^{2+} store in bullfrog sympathetic neurones modulates effects of Ca^{2+} entry on $[Ca^{2+}]_i$. *J. Physiol.* 450:217–246.
- Friel, D.D., and R.W. Tsien. 1992b. Phase-dependent contributions from Ca^{2+} entry and Ca^{2+} release to caffeine-induced $[Ca^{2+}]_i$ oscillations in bullfrog sympathetic neurons. *Neuron.* 8:1109–1125.
- Friel, D.D. 1998. Three modes of Ca^{2+} induced Ca^{2+} release in neurons. In *Information Processing in Cells and Tissues*. M. Holcombe and R. Paton, editors. Plenum Press, New York. 47–56.
- Hongpaisan, J., N.B. Pivovarova, S.L. Colegrove, D.D. Friel, and S.B. Andrews. 1999. Interactions between mitochondria and endoplasmic reticulum modulate Ca^{2+} signaling in sympathetic neurons. *Soc. Neurosci.* 25:1249. (Abstr.)
- Hongpaisan, J., N.B. Pivovarova, S.L. Colegrove, R.D. Leapman, D.D. Friel, and S.B. Andrews. 2001. Multiple modes of calcium-induced calcium release in sympathetic neurons II: A $[Ca^{2+}]_i$ and location-dependent transition from ER Ca accumulation to net Ca release. *J. Gen. Physiol.* 118:101–112.
- Hua, S.Y., M. Nohmi, and K. Kuba. 1993. Characteristics of Ca^{2+} release induced by Ca^{2+} influx in cultured bullfrog sympathetic neurons. *J. Physiol.* 464:245–272.
- Jack, J.J.B., D. Noble, and R.W. Tsien. 1983. *Electrical current flow in excitable cells*. Clarendon Press, Oxford.
- Jones, L.R., H.R. Besch, Jr., J.L. Sutko, and J.T. Willerson. 1979. Ryanodine-induced stimulation of net Ca^{++} uptake by cardiac sarcoplasmic reticulum vesicles. *J. Pharmacol. Exp. Ther.* 209:48–55.
- Khodakhah, K., and C.M. Armstrong. 1997. Inositol trisphosphate and ryanodine receptors share a common functional Ca^{2+} pool in cerebellar Purkinje neurons. *Biophys. J.* 73:3349–3357.
- Kuba, K. 1994. Ca^{2+} -induced Ca^{2+} release in neurons. *Jap. J. Physiol.* 44:613–650.
- Lipscombe, D., D.V. Madison, M. Poenie, H. Reuter, R.W. Tsien, and R.Y. Tsien. 1988. Imaging of cytosolic Ca^{2+} transients arising from Ca^{2+} stores and Ca^{2+} channels in sympathetic neurons. *Neuron.* 1:355–365.
- Llano, I., R. DiPolo, and A. Marty. 1994. Calcium-induced calcium release in cerebellar Purkinje neurones. *Neuron.* 12:663–673.
- Llano, I., J. Gonzalez, C. Caputo, F.A. Lai, L.M. Blayney, Y.P. Tan, and A. Marty. 2000. Presynaptic calcium stores underlie large-amplitude miniature IPSCs and spontaneous calcium transients. *Nat. Neurosci.* 3:1256–1265.
- Lytton, J., M. Westlin, S.E. Burk, G.E. Shull, and D.H. MacLennan. 1992. Functional comparisons between isoforms of the sarcoplasmic or endoplasmic reticulum family of calcium pumps. *J. Biol. Chem.* 267:14483–14489.
- Meldolesi, J., and T. Pozzan. 1998. The endoplasmic reticulum Ca^{2+} store: a view from the lumen. *Trends Biochem. Sci.* 23:10–14.
- Muschol, M., B.R. Dasgupta, and B.M. Salzberg. 1999. Caffeine interaction with fluorescent calcium indicator dyes. *Biophys. J.* 77:577–586.
- Narita, K., T. Akita, M. Osanai, T. Shirasaki, H. Kijima, and K. Kuba. 1998. A Ca^{2+} -induced Ca^{2+} release mechanism involved in asynchronous exocytosis at frog motor nerve terminals. *J. Gen. Physiol.* 112:593–609.
- Narita, K., T. Akita, J. Hachisuka, S.-M. Huang, K. Ochi, and K. Kuba. 2000. Functional coupling of Ca^{2+} channels to ryanodine receptors at presynaptic terminals. *J. Gen. Physiol.* 115:519–532.
- Neher, E., and G.J. Augustine. 1992. Calcium gradients and buffers in bovine chromaffin cells. *J. Physiol.* 450:273–301.
- Peng, Y.Y. 1996. Ryanodine-sensitive component of calcium transients evoked by nerve firing at presynaptic nerve terminals. *J. Neurosci.* 12:6703–6712.
- Pfaffinger, P.J., M.D. Leibowitz, E.M. Subers, N.M. Nathanson, W. Almers, and B. Hille. 1988. Agonists that suppress M-current elicit phosphoinositide turnover and Ca^{2+} transients, but these events do not explain M-current suppression. *Neuron.* 1:477–484.
- Pivovarova, N.B., J. Hongpaisan, S.B. Andrews, and D.D. Friel. 1999. Depolarization-induced mitochondrial Ca accumulation in sympathetic neurons: Spatial and temporal characteristics. *J. Neurosci.* 19:6372–6384.

- Pozzo-Miller, L.D., N.B. Pivovarova, R.D. Leapman, R.A. Buchanan, T.S. Reese, and S.B. Andrews. 1997. Activity-dependent calcium sequestration in dendrites of hippocampal neurons in brain slices. *J. Neurosci.* 17:8729–8738.
- Pozzan, T., R. Rizzuto, P. Volpe, and J. Meldolesi. 1994. Molecular and cellular physiology of intracellular calcium stores. *Physiol. Rev.* 74:595–636.
- Rousseau, E., J.S. Smith, and G. Meissner. 1987. Ryanodine modifies conductance and gating behavior of single Ca^{2+} release channel. *Am. J. Physiol.* 253:C364–C368.
- Rousseau, E., J. LaDine, Q.Y. Liu, and G. Meissner. 1988. Activation of the Ca^{2+} release channel of skeletal muscle sarcoplasmic reticulum by caffeine and related compounds. *Arch. Biochem. Biophys.* 267:75–86.
- Sandler, V.M., and J.G. Barbara. 1999. Calcium-induced calcium release contributes to action potential evoked calcium transients in hippocampal CA1 pyramidal neurons. *J. Neurosci.* 19:4325–4336.
- Shmigol, A., A. Verkhratsky, and G. Isenberg. 1995. Calcium-induced calcium release in rat sensory neurons. *J. Physiol.* 489:627–636.
- Sutko, J.L., J.A. Airey, W. Welch, and L. Ruest. 1997. The pharmacology of ryanodine and related compounds. *Pharmacol. Revs.* 49: 53–98.
- Thayer, S.A., L.D. Hirning, and R.J. Miller. 1988. The role of caffeine-sensitive calcium stores in the regulation of intracellular free calcium concentration in rat sympathetic neurons in vitro. *Mol. Pharmacol.* 34:664–673.
- Toescu, E.C. 1998. Intraneuronal Ca^{2+} stores act mainly as a Ca^{2+} sink; in cerebellar granule cells. *Neuroreport.* 9:1227–1231.
- Usachev, Y., and S.A. Thayer. 1997. All-or-none Ca^{2+} release from intracellular stores triggers by Ca^{2+} influx through voltage gates Ca^{2+} channels in rat sensory neurons. *J. Neurosci.* 17:7404–7414.
- Usachev, Y., and S.A. Thayer. 1999. Controlling the urge for a Ca^{2+} surge: all-or-none Ca^{2+} release in neurons. *Bioessays.* 21:743–750.
- Verkhratsky, A., and A. Shmigol. 1996. Calcium-induced calcium release in neurons. *Cell Calcium.* 19:1–14.
- Wei, H., W. Wenlin, D.E. Bredesen, and D.C. Perry. 1998. Bcl-2 protects against apoptosis in neuronal cell line caused by thapsigargin-induced depletion of intracellular calcium stores. *J. Neurochem.* 70:2305–2314.
- Zucchi, R., and S. Roncha-Testoni. 1997. The sarcoplasmic reticulum Ca^{2+} release channel/ryanodine receptor: modulation by endogenous effectors, drugs and disease states. *Physiol. Rev.* 49:1–51.